creative commons
COMMONS DEED

저작자표시-비영리-동일조건변경허락 2.0 대한민국

이용자는 아래의 조건을 따르는 경우에 한하여 자유롭게

- 이 저작물을 복제, 배포, 전송, 전시, 공연 및 방송할 수 있습니다.
- 이차적 저작물을 작성할 수 있습니다.

다음과 같은 조건을 따라야 합니다:

저작자표시. 귀하는 원저작자를 표시하여야 합니다.

비영리. 귀하는 이 저작물을 영리 목적으로 이용할 수 없습니다.

동일조건변경허락. 귀하가 이 저작물을 개작, 변형 또는 가공했을 경우에는, 이 저작물과 동일한 이용허락조건하에서만 배포할 수 있습니다.

- 귀하는, 이 저작물의 재이용이나 배포의 경우, 이 저작물에 적용된 이용허락조건을 명확하게 나타내어야 합니다.
- 저작권자로부터 별도의 허가를 받으면 이러한 조건들은 적용되지 않습니다.

저작권법에 따른 이용자의 권리는 위의 내용에 의하여 영향을 받지 않습니다.

이것은 이용허락규약(Legal Code)을 이해하기 쉽게 요약한 것입니다.

Disclaimer

dCollection

공학석사 학위논문

Fire Analysis of Cable-stayed Bridge Considering Wind Effect

바람의 영향을 고려한 사장교의 화재해석

2023 년 8 월

서울대학교 대학원

건설환경공학부

정 우 진

Fire Analysis of Cable-stayed Bridge Considering Wind Effect

바람의 영향을 고려한 사장교의

화재해석

지도 교수 김 호 경

이 논문을 공학석사 학위논문으로 제출함

2023년 08월

서울대학교 대학원

건설환경공학부

정 우 진

정우진의 공학석사 학위논문을 인준함

2023년 08월

위 원 장 _____ 송 준 호 _____ (인)

부위원장 _____ 김 호 경 _____ (인)

위 원 _____ 채 윤 병 _____ (인)

ABSTRACT

Fire Analysis of Cable-stayed Bridge Considering Wind Effect

Woo Jin Chung
Department of Civil and Environmental Engineering
Seoul National University

Design standards and countermeasures for cable-stayed bridges tend to focus on natural disasters such as earthquakes and typhoons. However, there remains a scarcity of research concerning the assessment criteria and guidelines for vehicle fires on these structures. Vehicle fires on cable-stayed bridges occur in open environments and are significantly influenced by wind. As a result, these factors warrant careful consideration during the evaluation of thermal fluid flow due to vehicle fires on cable-stayed bridges. The presence of wind can considerably affect the magnitude and extent of temperature changes in the cable components during a vehicle fire. Although prior studies have analyzed fire effects on cable-stayed bridges, none have incorporated wind effects.

The present study conducts a comprehensive thermal fluid analysis on cable-stayed bridges, accounting for potential wind effects. The analysis investigates temperature changes and threshold exceedance ranges in cables resulting from a vehicle fire. In addition, the study compares and evaluates temperature outcomes based on the presence or absence of wind. Considerations such as fire intensity, scenario configurations, and changes in material properties of cable components due to temperature variations are factored into the analysis. The Post-Tensioning Institute (PTI, 2012) standard serves as the reference for evaluating threshold exceedance ranges. The fire scenario includes factors such as vulnerable bridge sections, average wind speed, and fire suppression duration. A fire intensity model, suitable for vehicle fires in the open environment of cable-stayed bridges, is utilized. The thermal fluid analysis reveals that considering the wind's influence leads to a broader range of temperature exceedances for both the fire-occurring lane and the cables.

Keywords: Cable-stayed bridge, Thermal flow analysis, Vehicle Fire, Fire analysis.

Student Number: 2019-20019

TABLE OF CONTENTS

LIST OF FIGURES

LIST OF TABLES

CHAPTER 1

INTRODUCTION

1.1 Research Background and Trends

Disasters can be broadly categorized into natural calamities, such as earthquakes and typhoons, and societal catastrophes triggered by incidents like fires, explosions, and collisions involving maritime vessels or aircraft. Extensive research into natural disasters has led to the formulation of comprehensive design standards and preventative strategies for structures such as cable-stayed bridges. However, significant global events, notably the 9/11 terrorist attacks in the United States in 2001 and the train bombings in Spain in 2004, have highlighted the necessity of enhancing societal infrastructure resilience against threats like aircraft collisions, explosions, and fires. As illustrated in ‘(NYSDOT, 2017), bridge damage caused by fires, the most prevalent type of societal disaster, has been progressively increasing over time.

Table 1.1 Causes of failure as a percentage of total surveyed bridge failure (NYSDOT, 2017)

Causes of Failure	1980-1989	1990-1999	2000-2009	2010-2017	Total	Percentage
Hydraulic	162	246	93	71	572	46%
Overload	67	31	37	24	159	13%
Deterioration	26	22	23	4	75	6%
Construction Defects	3	11	1	0	20	2%
Earthquake	8	11	1	0	20	2%
Collision	57	55	51	47	210	17%
Fire	**8**	**10**	**12**	**22**	**52**	**4%**
Other	50	36	32	1	25	2%
SUM	381	422	259	195	1257	100%

The causative factors of bridge accidents are varied, encompassing scenarios such as lightning strikes, vehicle-induced fires, and tanker explosions. As represented in Table 1.2, among vehicular fires, those involving tank trucks—vehicles transporting hazardous substances with the potential to ignite fires or trigger explosions—are reported most frequently..

Table 1.2 Domestic and International Fire Accidents on Bridges

Bridge	Type	Years	Cause of fire
I-80W/I580E Highway Rich-mond	Steel girder	1995 (USA)	Tanker fire
Wonhyo	PSC girder	1996 (Korea)	Vehicle fire
I-20/I-59/I-65 Highway Alabama	Steel girder	2002 (USA)	Tanker fire
I-95 Howard Avenue	Steel girder	2003 (USA)	Tanker fire
Wiehltal	Plate girder	2004 (Germany)	Tanker fire
Bill Williams River	PSC girder	2006 (USA)	Tanker fire
Seohae	Cable-stayed	2006 (Korea)	Vehicle fire
Mezcala	Cable-stayed	2007 (Mexico)	Truck fire
MacArthur Maze	Plate girder	2007 (USA)	Tanker fire
Ikebukuro Sen	Plate girder	2008 (Japan)	Tanker fire
I-75 Highway Michigan	Steel girder	2009 (USA)	Tanker fire
Yangsan viaduct	PSC girder	2010 (Korea)	Tanker fire
Bucheon viaduct	Steel girder	2010 (Korea)	Tanker fire
60 Freeway in Montebello	PSC girder	2011 (USA)	Tanker fire
Merritt Island FL. SR528	PSC girder	2011 (USA)	Tanker fire
New Little Belt	Suspension	2013 (Denmark)	Truck fire
Zakim	Cable-stayed	2014 (USA)	Tanker fire
I-70 Highway Ohio	Concrete slab	2015 (USA)	Tanker fire
Seohae	Cable-stayed	2015 (Korea)	Lightning strike
Ambassador	Suspension	2015 (USA)	Tanker fire
Veterans Glass City Skyway	Cable-stayed	2015 (USA)	Tanker fire
Delaware Memorial	Suspension	2016 (USA)	Tanker fire
Ulsan	Suspension	2019 (Korea)	Tanker fire

Prince of Wales	Cable-stayed	2022 (UK)	Tanker fire
Crimea	Truss Arch	2022 (Russia)	Tanker fire
Gold Star Memorial	Steel Truss	2023 (USA)	Tanker fire
Port Mann	Cable-stayed	2023 (Canada)	Tanker fire

Fire incidents on bridges can originate from both the upper and lower structures. In conventional bridges, a fire starting from the lower section can cause significant damage to the upper superstructure and piers, including the girder.

(a) Zakim Bridge

(2014, USA)

(b) Veterans' Glass City Skyway Bridge

(2015, USA)

(c) Prince of Wales Bridge (2022, UK)   (d) Port Mann Bridge (2023, Canada)

Figure 1.1 Vehicle fire accidents on Cable-stayed bridge

Most long-span bridges, such as cable-stayed bridges, are strategically located over maritime areas, which can complicate vehicular access to their lower structures. Moreover, due to the expansive under-space of these bridges compared to traditional ones, fires starting in the lower structure are less likely to significantly impact the superstructure. However, vehicular fires that occur on the upper part of cable-stayed bridges could potentially have a substantial impact on the bridge's cable structures. Figure 1.1 presents an incident of a vehicle fire on a cable-stayed bridge. When a fire occurs on the upper part of a cable-stayed bridge, it can inflict considerable damage on the load-bearing cables. Thus, understanding the thermal characteristics of these cables and implementing effective fire resistance measures are pivotal for ensuring structural stability.

Currently, extensive research and technological advancements are underway, both domestically and globally, to develop fire countermeasures for cable-stayed bridges. However, there is a conspicuous lack of established guidelines and standards explicitly addressing fire-related incidents on such structures. Presently, fire-related standards and guidelines predominantly target buildings, with limited application to infrastructural entities like tunnels and traditional bridges. Tables 1.3 and 1.4 compile these fire-related standards from various jurisdictions. As previously outlined, fires originating from the upper sections of cable-stayed bridges can inflict considerable damage, thus underscoring the urgent need for effective fire countermeasures, particularly for the cables. Protective measures like fireproof blankets and fire-resistant covers have been devised to shield cables from fires, yet their implementation is rare, mainly due to the associated high costs. This situation necessitates further research to devise fire standards and guidelines that capture fire characteristics in the open areas of cable-stayed bridges, alongside studies on the optimal sections for reinforcing cable fireproofing.

Chung et al. (2019) offered insights into the fire intensities for different types of vehicles in open environments on cable-stayed bridges, and conducted evaluations on cable temperature variations due to vehicle fires. However, this study did not take into account the impact of wind. More recent research carried out heat transfer analyses on cable-stayed bridges exposed to vehicle fires, thereby assessing the effect of firewalls as a preventive measure on cable temperatures. Yet, this study did not extend its investigation to cable-stayed bridges.

Table 1.3 Domestic fire standards and guidelines

Domestic fire standards and guidelines
Building Code Enforcement Regulations Article 3 and 4 on evacuation and fire safety measures of buildings (Ministry of Land, Infrastructure, and Transport Decree No. 1106, 2022. 02. 11.)
Enforcement decree of Building Act, Article 56 and 57 (Presidential Decree No. 32411, 2022. 02. 11.)
Fire Protection Design Guidelines for the Underside of Highway Bridges (Korea Expressway Corporation, 2014)
Guidelines for Fire Risk Assessment of Highway Bridges (Korea Expressway Corporation, 2014)
Ventilation and Disaster Prevention Standards for Highway Tunnels (Korea Expressway Corporation, 2012)
Management Standards for Fire Resistance Performance of High-strength Concrete Columns and Beams (Ministry of Land, Infrastructure and Transport Notification No. 2008-334, 2008. 07. 21.)
Recognition and Management Standards for Fire-Resistant Structures (Ministry of Land, Infrastructure and Transport Notification No. 2016-416, 2016. 08. 01.)
Fire Protection Guidelines for Road Tunnels (Ministry of Land, Infrastructure and Transport, 2021)
Guidelines for the Installation and Management of Disaster Prevention Facilities in Road Tunnels (Ministry of Land, Infrastructure and Transport, 2016)
Fire Safety Standards for Road Tunnels (NFSC 603) (National Fire Agency, 2017)
Design Guidelines for Urban Underground Roads (Ministry of Land, Infrastructure and Transport, 2016)
Fireproof Design and Construction Guidelines for Tunnels (Korea Expressway Corporation, 2013)

Table 1.4 International fire standards and guidelines

International fire standards and guidelines
Europe, Eurocode 1: Actions on structures – Part 1-2: General actions – Actions on structures exposed to fire (CEN, 2002)
Europe, Eurocode 2: Design of concrete structures – Part 1-2: General rules – Structural fire design (CEN, 2004)
Europe, Eurocode 3: Design of steel structures – Part 1-2: General rules – Structural fire design (CEN, 2005)
France, Centre d'Etudesdes Tunnel(Tunnel Design Center) (CETU, 2002)
Germany, German Standards Fire Resistance Tests (DIN 4102, 1977)
Germany, Richtilinien fur die Ausstattung und den Betrieb von StraBentunneln (RABT, 2006)
ISO 834-1, Fire-resistance tests-Elements of building construction-Part 1: General re-quirements (ISO, 1999)
ITA, Guidelines for Structural Fire Resistance for Road Tunnels (ITA, 2004)
ITA, Structural Fire Protection For Road Tunnels (ITA, 2017)
PIARC, PIARC Proposal on the Design Criteria for Re-sistance to Fire to Road Tunnel Structures (PIARC, 2002)
PIARC, Fire and Smoke Control in Road Tunnels (PIARC, 2007)
PTI, Recommendations for Stay Cable Design, Testing, and Installation (PTI, 2012)
Sweden, Svensk Bygg Norm 67 (BABS, 1967)
USA, ACI 216/TMS-0216 Code Requirements for Determining Fire Resistance of Con-crete and Masonry Construction Assemblies (ACI, 2007)
USA, ACI 216 Guide for Determining the Fire Endurance of Concrete Elements (ACI, 1989)

USA, ASTM E119-82 (Standard Methods of Fire Tests of Building Construction and Materials) (ASTM, 2000)
USA, NFPA 502 Standard for Road Tunnels, Bridges, and Other (NFPA, 2017)

1.2 Objective and Scope

Despite the ongoing incidence of vehicle-induced fires on cable-stayed bridges, the existing countermeasures are evidently insufficient. Considering the characteristics of vehicle fires, one potential countermeasure for cable-stayed bridges could be the use of fireproof blanket protective covers to safeguard cables located in high-risk fire sections. However, given the substantial costs associated with their installation on operational bridges, it is vital to conduct comprehensive research and establish detailed guidelines regarding the extent of such protective measures. To achieve this, an initial assessment of temperature characteristics arising from vehicle fires on cable-stayed bridges, with an emphasis on the influence of wind, is a critical requirement.

In this investigation, thermal fluid analyses were carried out using FDS v6.7.6 (NIST, 2021), considering both an appropriate fire intensity model in the context of the open environment of cable-stayed bridges, and the significant influence of wind during fire incidents. By utilizing thermal fluid analyses, this research derived the temperature-time histories for cables, thereby enabling an exploration of the potential maximum temperatures that cables might reach during vehicle fires, the range exceeding temperature criteria, the contact range, and the wind's influence on the affected lanes. The findings from this study are expected to provide valuable evaluation data for determining fire countermeasures and the scope of fireproof reinforcement required for cables on cable-stayed bridges in the event of vehicle fires.

The key research contributions of this paper are as follows:

Chapter 1 outlines the research background, the scope, and the objectives of this paper.

Chapter 2 compiles methodologies for analyzing vehicle fires on cable-stayed bridges, taking into account the effects of wind. It elaborates on the characteristics of vehicle fires on bridges, fire scenarios specific to cable-stayed bridges, and the thermal properties of structural steel during fires.

Chapter 3 presents the methodologies for conducting thermal transfer analyses on cable-stayed bridges. It outlines the criteria for examining temperatures produced in cables during vehicle fires and the analysis methods accounting for the presence or absence of wind impact. The chapter includes essential aspects for achieving the main objective of the paper—verifying fire simulations with FDS, numerical analysis models, analysis conditions, and analysis cases pertinent to thermal fluid analysis using FDS-smv—all while considering the influence of wind.

Chapter 4 details the findings from the thermal fluid analyses of cable-stayed bridges, considering the presence or absence of wind impact, and categorizes the results according to key variables.

Chapter 5 summarizes the conclusions derived from this study.

CHAPTER 2

FIRE ANALYSIS METHOD

This chapter details the fire analysis process and the criteria for selecting an appropriate fire intensity model, specifically tailored for addressing vehicle fires that can potentially occur on the superstructures of cable-stayed bridges. This involves the analysis of several factors such as the design intensity for different types of vehicles and the effects of heat transfer during a vehicle fire, which are critical in determining a suitable fire intensity model for thermal fluid analysis. In addition, the chapter outlines the strategy for configuring fire scenarios and presents an overview of the material properties of the bridge cables, often constructed from structural steel.

2.1 Fire Analysis Procedure for Cable-stayed Bridge

The fire analysis procedure specifically intended for cable-stayed bridges is briefly presented in Figure 2.1 and encompasses the following key stages:

Initially, the target bridge and its fire-prone sections are identified. Next, potential scenarios of vehicle fires on the chosen bridge are examined, and appropriate fire intensity models are established. This process also includes setting representative wind speeds and directions to account for the potential influence of wind during the analysis. In the third stage, for application in the thermal fluid analysis, variations in the material properties of the cable due to temperature changes (specific heat, thermal conductivity), fire load (based on the fire intensity model), and boundary conditions are determined. Analytical cases are set up to evaluate the influence of wind during a vehicle fire. Finally, the thermal fluid analysis results are used to analyze temporal temperature changes in the cable, the extent of flame contact, and the range of lanes exceeding the defined standards based on the presence or absence of wind. The outcomes facilitate the verification of the range of standards exceeded by the cable.

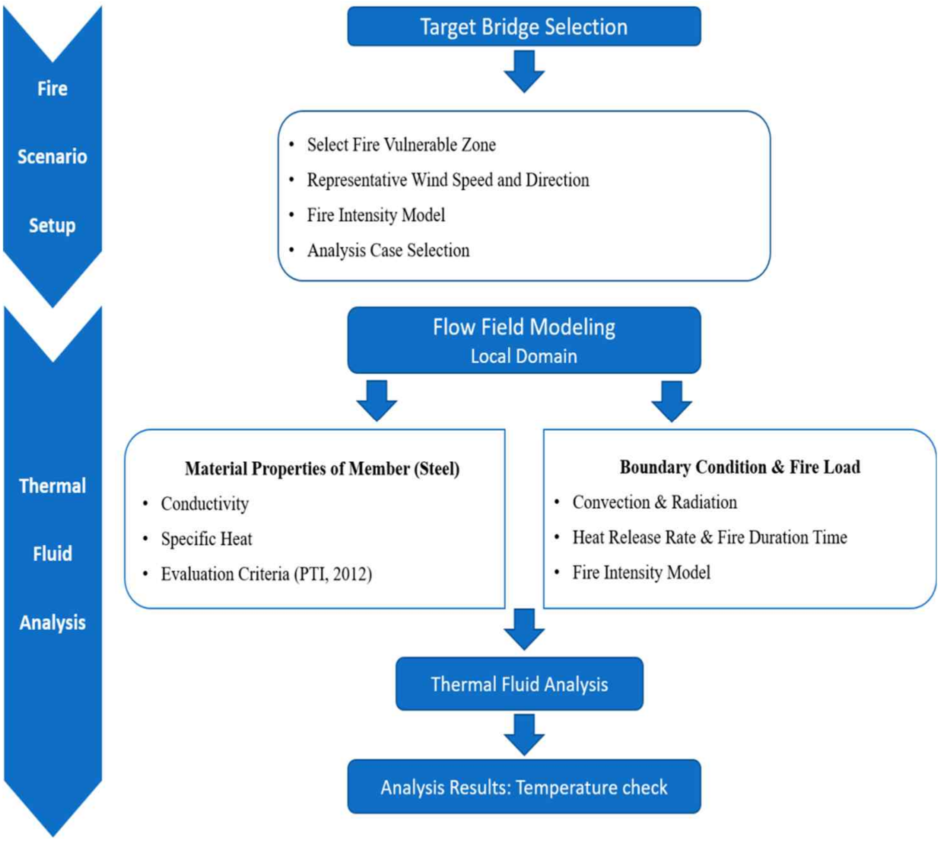

Figure 2.1 Fire analysis procedure for cable-stayed bridge

2.2 Fire Intensity Model

This section involves analyzing factors such as fire intensity based on vehicle type, as suggested by domestic and international fire-related standards, results from real-world vehicle fire experiments, and heat transfer effects during a vehicle fire. This comprehensive analysis aids in determining a fire intensity model that is suitable for application in a thermal fluid analysis for the relatively open environment of cable-stayed bridges.

Currently, neither domestic nor international guidelines or standards are available that specifically address fires on bridge superstructures. As noted in Chapter 1, the majority of fire-related standards and guidelines cater to enclosed environments like buildings and tunnels. The commonly used ISO-834 standard fire curve (ISO, 1999), designed for buildings, and the RABT standard fire curve (RABT, 2006), intended for tunnels, is depicted in Figure 2.2. Notably, several studies have employed these two fire curves to evaluate the impacts of fire on bridge structures (Payá Zaforteza and Garlock, 2012; Yun and Jeon 2018; Kodur and Naser 2019).

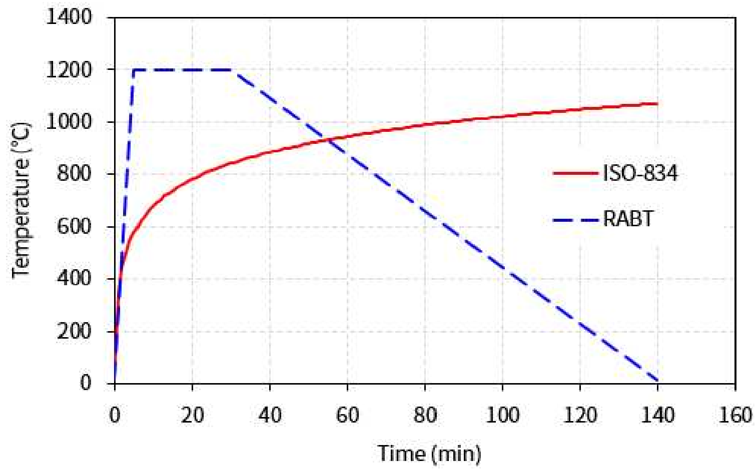

Figure 2.2 ISO 834 Standards fire curve and RABT Standards fire Curve

Typically, criteria for vehicular fires are defined by heat release rates specific to various vehicle types, rather than by the temperature-time curves previously mentioned. As shown in Table 2.1, the Korean Ministry of Land, Infrastructure, and Transport's 2016 Guidelines for the Installation and Management of Fire Protection Facilities in Road Tunnels present fire intensity design parameters for different vehicle types. However, they do not provide standards for heat release per unit area. In contrast, the U.S. standards for road tunnels (NFPA, 2017), as depicted in Table 2.2, prescribe heat release rates, unit areas, and maximum temperatures for distinct types of vehicles.

Table 2.1 Korean road tunnel fire resistance standards (Ministry of Land, Infrastructure, and Transport, 2016)

Cause of Fire	Equivalent Size of Gasoline Pool (m^2)	Fire HRR (MW)	Smoke Generation Rate (m^3/s)	Maximum Temperature (°C)
Passenger Car	-	~5	20	-
Bus	-	20	60-80	-
HGV	-	30	80	-
Tanker	-	100	200	-

Table 2.2 U.S. road tunnel fire resistance standards (NFPA 502, 2004)

Cause of Fire	Equivalent Size of Gasoline Pool (m^2)	Fire HRR (MW)	Smoke Generation Rate (m^3/s)	Maximum Temperature (°C)
Passenger Car	2	5	20-30	400
Bus	8	20	60-80	700
HGV	8	20-30	60-80	1000
Tanker	30-100	100	100-300	1,200-1400

The majority of fires in buildings and tunnels are predominantly indoor fires. Therefore, the proposed standards take into consideration the dynamics of fires within enclosed environments, where heat transfer typically occurs via convection and radiation. However, fires arising in the superstructures (upper parts) of bridges happen in more open environments, meaning that the heat transfer is primarily due to radiation. Furthermore, these fires are expected to have lower intensity compared to those in enclosed spaces. Hence, it's inferred that these standards might not be entirely applicable for addressing vehicle fires on cable-stayed bridges.

The Korean Institute of Bridge and Structural Engineers has put forth a fire intensity model to emulate vehicle fires in open spaces, as illustrated in Figure 2.3. This study uses the model from Figure 2.3 to perform thermal fluid analysis. To simulate realistic vehicle fires, fire sizes are designated according to vehicle types. The average length and width of each vehicle type, suggested by the Guidelines for Installation and Management of Fire Protection Facilities in Road Tunnels (Ministry of Land, Infrastructure, and Transport, 2016) and the Road Structure Rules (Ministry of Land, Infrastructure, and Transport, 2021), were used to calculate the fire size. The fire sizes and intensities for each vehicle type are compiled in Table 2.3.

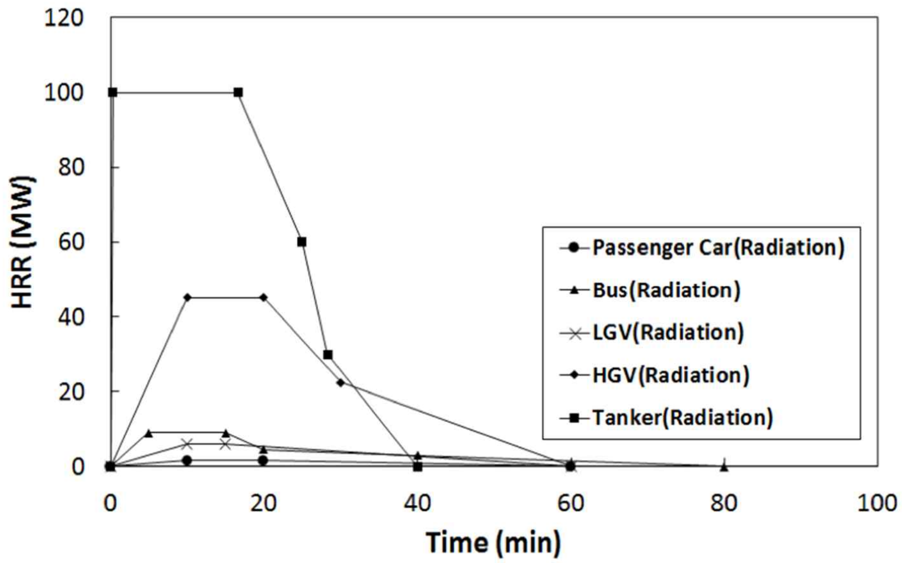

Figure 2.3 Fire Intensity Model (KIBSE, 2021)

Table 2.3 The fire sizes and intensities for each vehicle type

Type of Vehicle	HRR (Heat Release Rate)	Area (L X M)
Passenger Car	1.5 MW	4.3 m x 1.7 m
Bus	9.0 MW	10.7 m x 2.5 m
LGV	6.0 MW	4.5 m x 2.0 m
HGV	45.0 MW	6.1 m x 2.5 m
Tanker	100.0 MW	8.7 m x 2.5 m

2.3 Fire Scenario

This section discusses the method for establishing a fire scenario necessary for the thermal fluid analysis in this study. The process involves selecting the bridge of interest, identifying its fire-prone sections, choosing the representative wind speed and direction for the selected bridge, and taking into account the estimated time for fire suppression following a vehicle fire outbreak. These factors are considered in designing a fire scenario compatible with the fire intensity model.

2.3.1 Target Bridge and Fire Location

The Seohae Grand Bridge was chosen for examination in this study. This marine bridge forms part of the West Coast Expressway and connects Dangjin City in Chungcheongnam-do to Pyeongtaek City in Gyeonggi-do. The bridge has a total length of 990 meters (60.0 + 200.0 + 470.0 + 200.0 + 60.0) and is structured as a five-span continuous bridge with its main span measuring 470 meters. Comprising two types of steel box girders and a precast concrete deck, the bridge attains an impressive width of 34 meters.

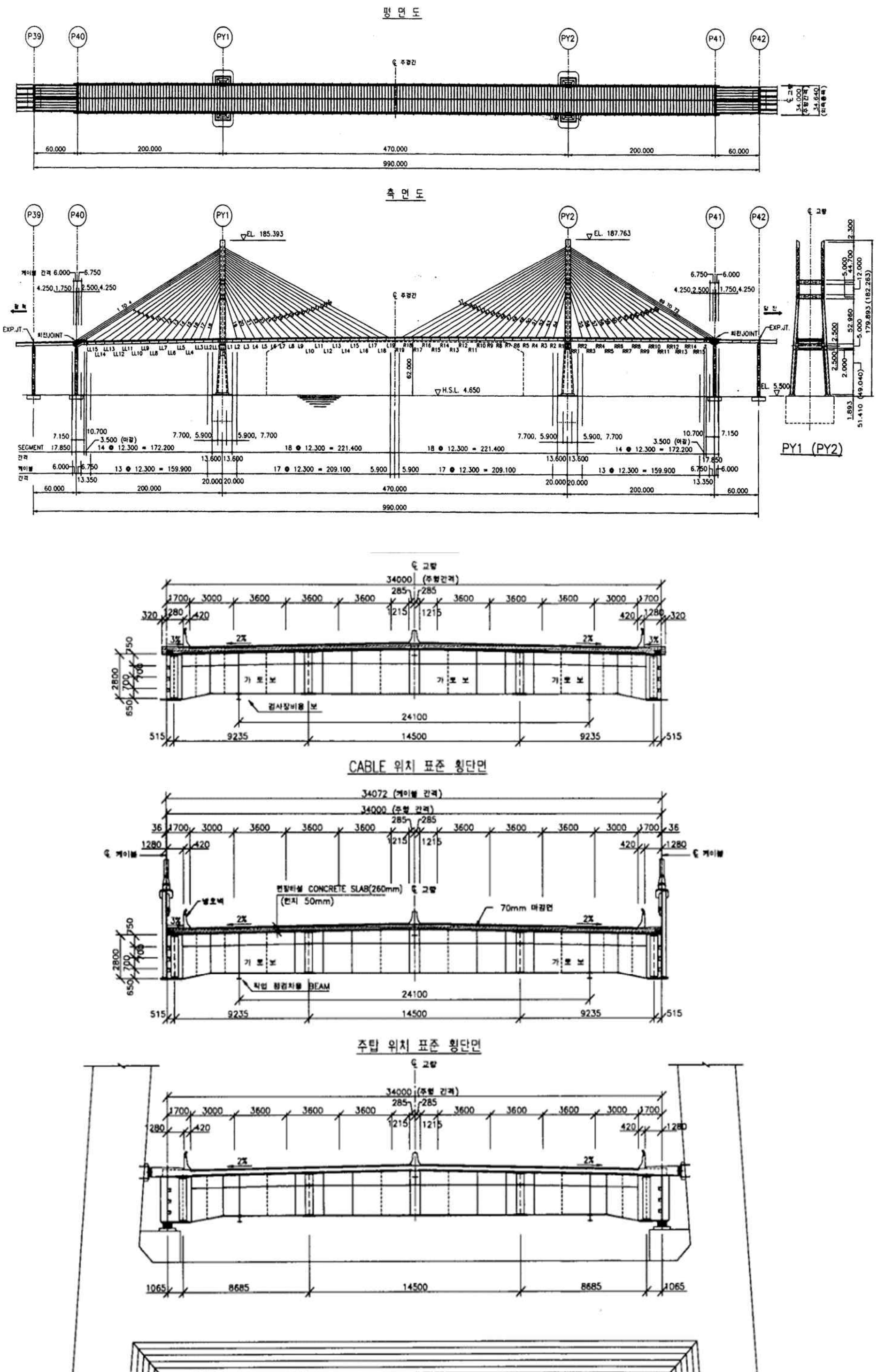

Figure 2.4 Target bridge overview

Korean Institute of Bridge and Structural Engineers (as referred to in the KIBSE report) conducted a thermal transmission analysis on the Seohae Grand Bridge, focusing on scenarios involving vehicle fires. This analysis allowed them to assess temperature fluctuations in the cables during such incidents. Based on these findings, they evaluated the potential risk areas (heights) for cables where the resulting temperatures exceeded the standards set by the Post-Tensioning Institute (PTI, 2012).

Utilizing a fire intensity model discussed in Section 2.2, they simulated fires in open spaces and conducted a thermal transmission analysis. This analysis accounted for radiant heat from a fire source located at a specified distance from the structure. Sections of the cables, distinguished by their maximum ($0.013m^2$) and minimum ($0.005m^2$) cross-sectional areas, were identified for this thermal transmission analysis. The results indicated that the temperature of the cables with the smallest cross-sectional area exceeded the PTI standard temperature only in scenarios involving a tanker truck fire on the bridge's shoulder. These findings are illustrated in Figure 2.6. For the cables with the maximum cross-sectional area, the temperature did not exceed the PTI temperature standard of 300 degrees, as displayed in Figure 2.7. It's important to note that these results did not factor in wind effects.

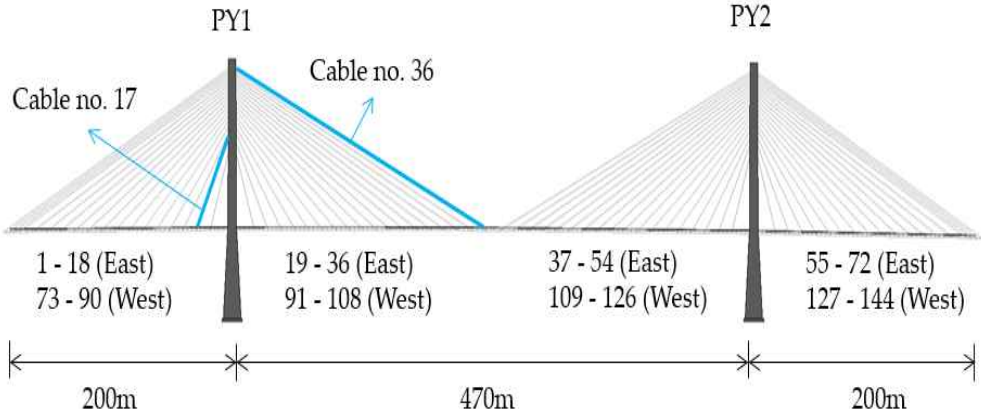

Figure 2.5 Target Bridge and cables (KIBSE 2021)

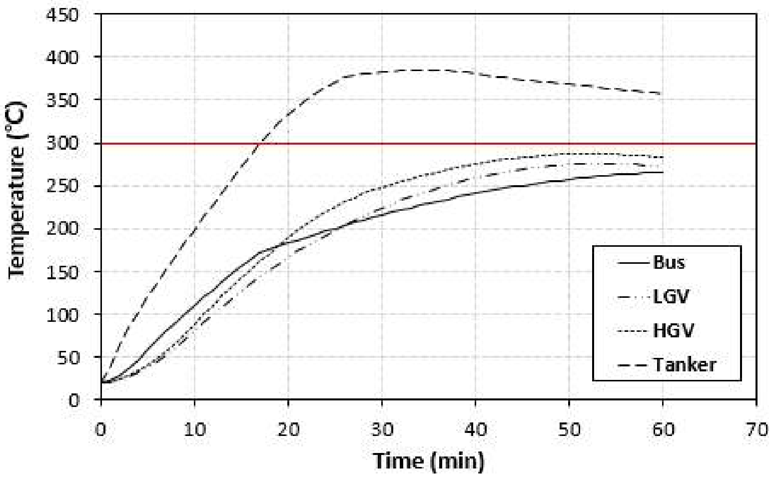

Figure 2.6 Analysis Results for the Minimum Cross-Sectional Area of Cables 17 during a Shoulder Fire (KIBSE, 2021)

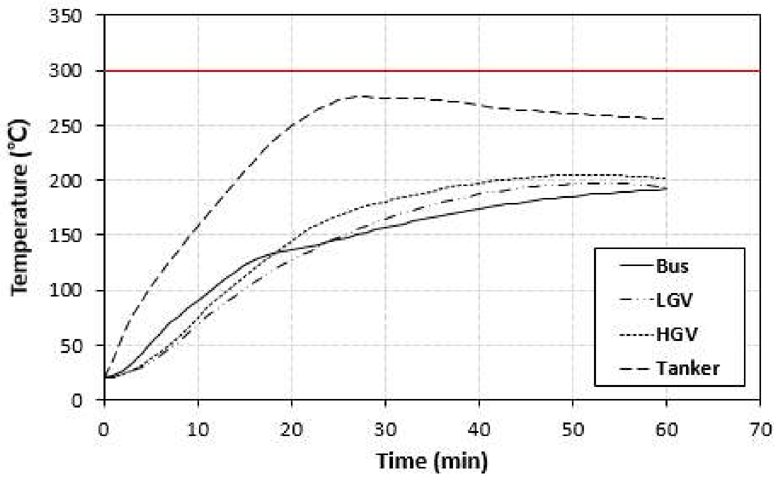

Figure 2.7 Analysis Results for the Maximum Cross-Sectional Area of Cables 36 during a Shoulder Fire (KIBSE 2021)

This study highlights the central span as the area most susceptible to vehicle fires (as depicted in Figure 2.8). This section's relative flatness, in contrast to the side spans, results in a broader impact range of a fire on the cables. With this in mind, the central span, where cables 34-36 (characterized by maximum cross-sectional areas) are situated, was designated as the area most prone to fire hazards.

Drawing upon previous studies, which used fire intensities associated with various types of vehicles (**as depicted in Figure 2.3**), it was observed that temperatures exceeding PTI's guidelines only occurred on cables with the smallest cross-sectional areas during instances of a tanker truck fire on the bridge's shoulder.

Thus, this research focuses predominantly on the analysis of tanker truck fires, comparing the resultant temperatures in scenarios with and without wind. The wind speed considered for this analysis was 3.8m/sec, in accordance with the Seohae Grand Bridge Fire Response Manual (2002).

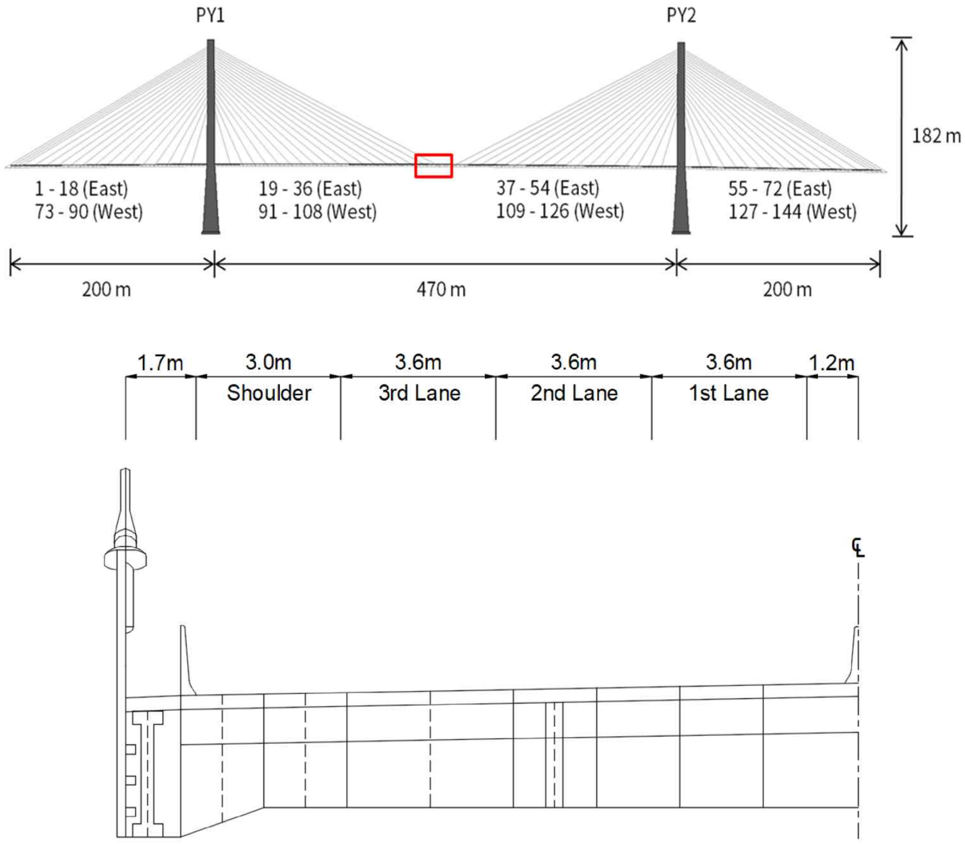

Figure 2.8 Fire location and cross-sectional view

2.3.2 Representative Wind Speed and Direction

The thermal fluid analysis in this study applied a representative wind speed of 3.8m/s, based on the average wind speed suggested for the Seohae

Grand Bridge in the 2002 Fire Response Manual. The primary wind direction utilized for analysis was determined using real-time measurement data from the Seohae Grand Bridge in 2021, which incorporated the 10-minute average wind speed and direction. This is depicted in Figures 2.10. The figures demonstrate that the dominant wind direction tends to fall within a specific range, primarily aligned perpendicular to the bridge axis. However, in the context of a vehicle fire, this study designates the wind direction perpendicular to the bridge axis. This direction is predicted to have the most significant impact on the increase in cable temperatures during such incidents.

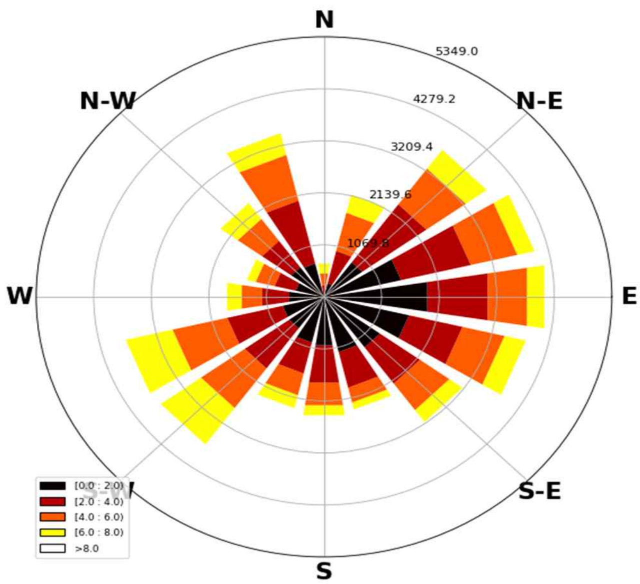

Figure 2.9 Wind Rose using real-time measurement data from Seohae Bridge

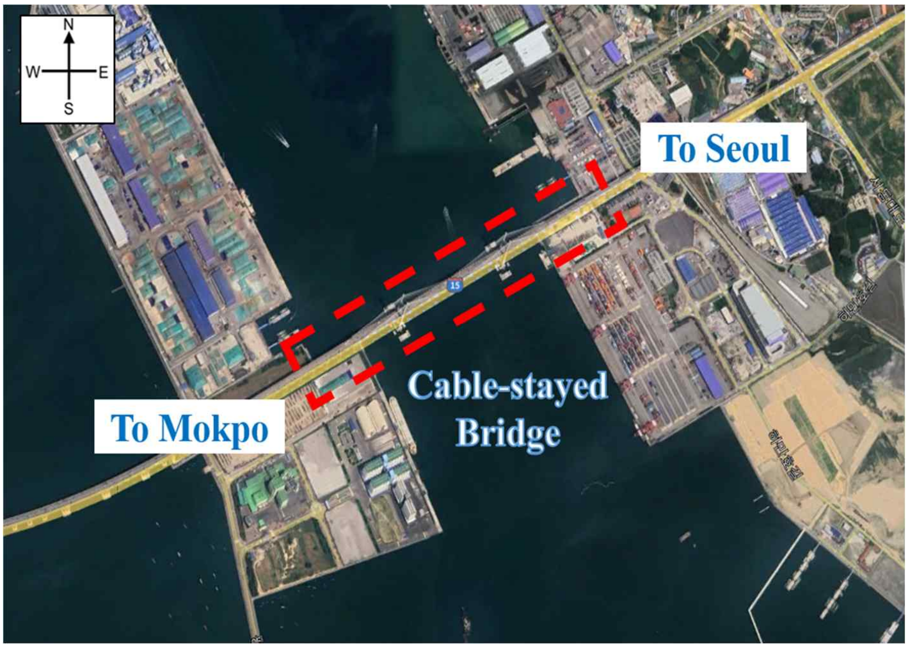

Figure 2.10 Target bridge aerial view

2.4 Thermal Characteristics of the Cable

This study applies the thermal properties of steel to cables, allowing for these properties to change according to temperature. The specific heat and thermal conductivity of steel were obtained using the formulas stipulated in EUROCODE 3 (referenced from 2005 documentation). The EUROCODE 3 provides guidelines for determining specific heat (refer to Equation 2.1) and thermal conductivity (refer to Equation 2.2).

$$20℃ \leq \theta_a < 600℃ : c_a = 425 + 7.73 \times 10^{-1}\theta_a - 1.69 \times 10^{-3}\theta_a^2 + 2.22 \times 10^{-6}\theta_a^3 \text{ (J/kg℃)}$$

$$600℃ \leq \theta_a < 735℃ : c_a = 666 + \frac{13002}{738 - \theta_a} \ (\text{J/kg℃})$$

$$735℃ \leq \theta_a < 900℃ : c_a = 545 + \frac{17820}{\theta_a - 731} \ (\text{J/kg℃}) \qquad (2.1)$$

$$900℃ \leq \theta_a \leq 1200℃ : c_a = 650 \ (\text{J/kg℃})$$

$$T \leq 800℃ : k_s = 54 - \frac{T}{30} \ (\text{W/m℃}) \qquad (2.2)$$

$$T > 800℃ : k_s = 27.3 \ (\text{W/m℃})$$

Changes in specific heat and thermal conductivity, as suggested by EUROCODE 3, corresponding to temperature increases are illustrated in Figure 2.11.

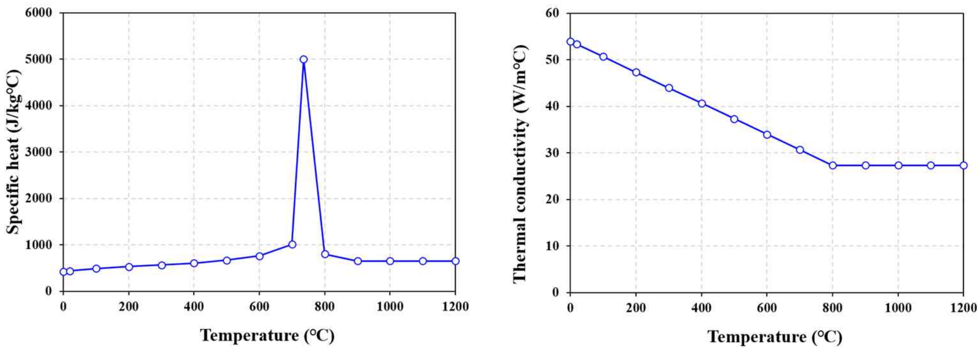

(a) Specific Heat (b) Thermal Conductivity

Figure 2.11 Specific heat and thermal conductivity as proposed in EUROCODE 3 (EN 1993-1-2, 2005)

CHAPTER 3

HEAT TRANSFER ANALYSIS IN CABLES

3.1 Heat Transfer Analysis Methods and Temperature Benchmark Criteria

There are two primary techniques for the analysis of vehicle fires on bridges. The first involves using a volumetric radiation model to calculate thermal loads through heat flux. The heat flux represents the energy flow per unit surface area, which arises from radiated heat impacting an element situated at a specific distance. The second technique employs a thermal fluid analysis via Computational Fluid Dynamics (CFD). The most notable example of this is the Fire Dynamic Simulator (FDS), developed by the U.S. National Institute of Standards and Technology (NIST). The FDS v6.7.6 (NIST, 2021) primarily focuses on predicting the flow of heat and smoke from fires and performs calculations based on the Navier-Stokes equations as part of a CFD analysis. FDS v6.7.6 (NIST, 2021) can assess large-scale thermal fluid phenomena that are not feasible to investigate experimentally and can effectively simulate diverse events such as heat and smoke generation from a fire, as well as the radiative and convective heat exchange between the environment and structures.

The technique that employs the volumetric radiation model does not consider the effects of wind, thus requiring the thermal fluid analysis method for fire analysis to account for the impact of wind. In this research, to incorporate wind effects, fire analysis was conducted using FDS v6.7.6 (NIST, 2021). The vehicular fire intensity model applied in the analysis was derived from the fire intensity demonstrated in Figure 2.4.

As per the PTI standards, it should take no less than 30 minutes for the temperature to reach 300 degrees Celsius on the external surface of a cable. In other words, cables that have undergone fireproofing should demonstrate fire resistance for at least 30 minutes. Moreover, it is mandated that the anchorage components should resist failure or slippage for at least 30 minutes in scenarios where a fire load of a minimum of 300 degrees Celsius and a tensile force corresponding to 45% of the cable's tensile strength act simultaneously.

The 'Guide for Determining the Fire Endurance of Concrete Element' by the ACI Committee 216 (ACI, 1989) proposes the variation in strength with increasing temperature for specific types of steel, as depicted in Figure 2.9. The steel utilized in the cables of the Seohae Grand Bridge (Parallel Strand (BS 5896: Super Grade [Class 2]) maintains about 75% of its tensile strength at 300 degrees Celsius. However, considering the ignition point of the high-density polyethylene (HDPE) tube encasing the cable components is 300 degrees Celsius, the benchmark temperature for this study was established at

300 degrees Celsius, measured from the surface of the cable.

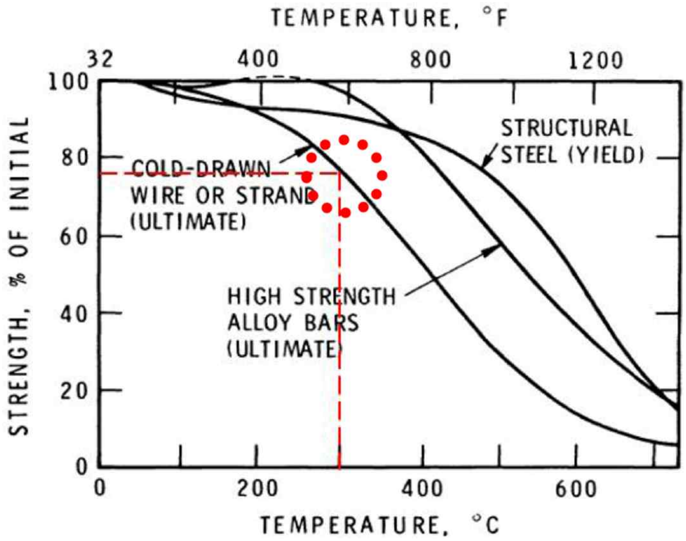

Figure 3.1 Strength of Certain Steels at High Temperatures (ACI, 1989)

3.2 Heat Transfer Analysis Leveraging the Volumetric Radiative Heat Source Model

The model for vehicle fire intensity is employed to determine the heat load, which is calculated as the heat flux. Heat flux represents the energy flow per unit surface area over time, stemming from radiant heat impacting a structure positioned at a particular distance. This strategy is crucial for executing the heat transfer analysis of cable bridges, facilitating the estimation of temperature changes in the cable bridge induced by vehicle fires. The progression of fire analysis following this methodology is as follows:

(1) Estimation of Heat Flux

The heat flux transmitted to a structure positioned at a specific distance is computed using equation (3.1).

$$q' = E \times F_{12} \tag{3.1}$$

Where,

q' : Heat flux (kW/m^2)

E : Emissive power (kW/m^2)

F_{12} : Configuration factor

(2) Evaluation of Emissive Power

The emissive power, quantified as the radiant heat emission from a unit surface area over a unit time span, is calculated with equation (3.2). This calculation presumes the flame as a cylindrical black body (Shokri, 1989).

$$E = 58 \times 10^{-0.00823\ D} \tag{3.2}$$

$$D = \sqrt{4A_f/\pi} \tag{3.3}$$

Where,

D :: Diameter of the flame (m)

A_f : Flame area (m^2)

(3) Calculation of Configuration Factor for the Flame

The configuration factor signifies the ratio of thermal energy entering from one surface to that exiting from another surface. Its value ranges from 0 to 1, depending on the distance between the target object and the flame. Figure 3.1 portrays the relationship between an idealized cylindrical flame and the target. As illustrated in Figure 3, the height of the idealized flame is calculated using equation (3.4), as indicated by Heskestad, 1983.

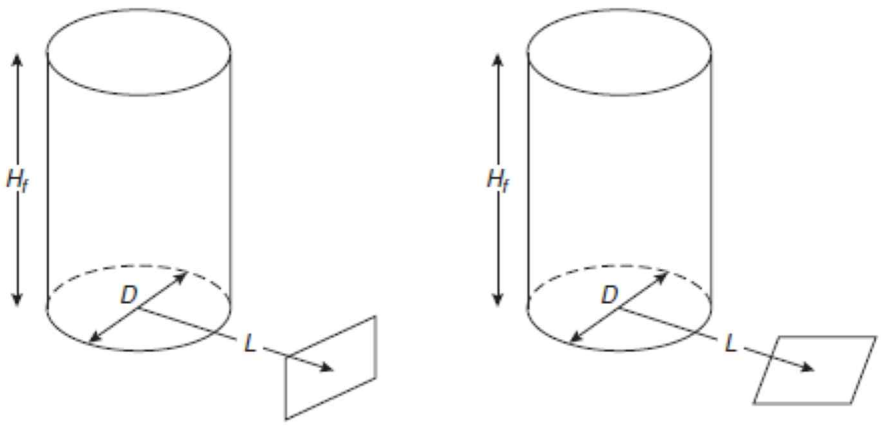

(a) Scenario with the target situated on the ground

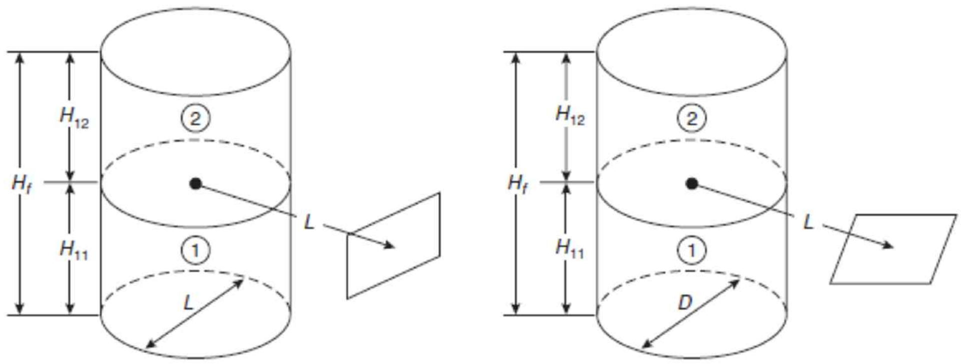

(b) Scenario with the target positioned above the ground

Figure 3.2 Relationship between the target and an idealized cylindrical flame (Beyler, 2002)

$$H_f = 0.235Q^{2/5} - 1.02D \tag{3.4}$$

Where,

H_f : Flame height (m)

Q : Flame heat release rate (kW)

D : Flame diameter (m)

As shown in Figure 3(a), when the target is on the ground, the configuration factors for the horizontal and vertical planes of the target are determined using equations (3.5) and (3.6).

$$F_{12,H} = \frac{B-\frac{1}{S}}{\pi\sqrt{B^2-1}}\tan^{-1}\sqrt{\frac{(B+1)(S-1)}{(B-1)(S+1)}} - \frac{A-\frac{1}{S}}{\pi\sqrt{A^2-1}}\tan^{-1}\sqrt{\frac{(A+1)(S-1)}{(A-1)(S+1)}} \quad (3.5)$$

$$F_{12,V} = \frac{1}{\pi S}\tan^{-1}\left(\frac{h}{\sqrt{S^2-1}}\right) - \frac{h}{\pi S}\tan^{-1}\sqrt{\frac{S-1}{S+1}} + \frac{Ah}{\pi S\sqrt{A^2-1}}\tan^{-1}\sqrt{\frac{(A+1)(S-1)}{(A-1)(S+1)}} \quad (3.6)$$

Where,

$F_{12,H}$: Configuration factor of the target's horizontal surface

$F_{12,V}$: Configuration factor of the target's vertical surface

$A = \frac{h^2+S^2+1}{2S}$

$B = \frac{1+S^2}{2S}$

$S = \frac{2L}{D}$

$h = \frac{2H_f}{D}$

L : Distance from the center of the flame to the target (m)

H_f : Flame height (m)

D : Flame diameter (m)

Considering both the horizontal and vertical configuration factors, the maximum configuration factor is determined by the vector sum of these values.

$$F_{12,max} = \sqrt{F_{12,H}^2 + F_{12,V}^2} \tag{3.7}$$

As shown in Figure 3(b), when the target is above the ground, the vertical configuration factor of the target can be determined by dividing the target point into upper and lower sections relative to the flame, as depicted by equations (3.8a), (3.8b), and (3.9).

$$F_{12,V1} = \frac{1}{\pi S}\tan^{-1}\left(\frac{h_1}{\sqrt{S^2-1}}\right) - \frac{h_1}{\pi S}\tan^{-1}\sqrt{\frac{(S-1)}{(S+1)}} - \frac{A_1 h_1}{\pi S\sqrt{{A_1}^2-1}}\tan^{-1}\sqrt{\frac{(A_1+1)(S-1)}{(A_1-1)(S+1)}} \tag{3.8a}$$

$$F_{12,V2} = \frac{1}{\pi S}\tan^{-1}\left(\frac{h_2}{\sqrt{S^2-1}}\right) - \frac{h_2}{\pi S}\tan^{-1}\sqrt{\frac{(S-1)}{(S+1)}} - \frac{A_2 h_2}{\pi S\sqrt{{A_2}^2-1}}\tan^{-1}\sqrt{\frac{(A_2+1)(S-1)}{(A_2-1)(S+1)}} \tag{3.8b}$$

$$F_{12,V} = F_{12,V1} + F_{12,V2} \tag{3.9}$$

Where,

$S = \frac{2L}{D}$

$h_1 = \frac{2H_{f1}}{D}$

$$A_1 = \frac{{h_1}^2 + S^2 + 1}{2S}$$

$$h_2 = \frac{2H_{f2}}{D}$$

$$A_2 = \frac{{h_2}^2 + S^2 + 1}{2S}$$

(4) Computation of Heat Flux

Steps (1) through (3) lead to the calculation of heat flux, which is then utilized to perform the heat transfer analysis.

(5) Conducting the Heat Transfer Analysis

The heat transfer analysis is carried out using the heat flux values acquired from steps (1) to (4). In this analysis, the properties of the cable are considered by taking into account the thermal properties of steel and their variations with temperature.

3.3 Thermal Fluid Analysis via the Fire Dynamic Simulator (FDS)

The present research conducted a thermal fluid analysis of cable components in cable-stayed bridges, focusing specifically on their exposure to vehicular fires. Utilizing FDS v6.7.6 (NIST, 2021), we estimated the temperature fluctuations within these cable components during a vehicular fire, considering both the presence and absence of wind.

3.3.1 FDS Fire Simulation Verification

Models for numerically simulating fire phenomena are broadly classified into two primary categories, as depicted in Figure 3.2. The first, referred to as the Zone model, divides the study area into an upper and lower layer for computation, as shown in Figure 3.3(a). This model is predominantly employed when predicting the effects of fire growth within enclosed spaces, such as building interiors. The second category, known as the Field model, partitions the target space into numerous control volumes, utilizing Computational Fluid Dynamics (CFD) techniques to analyze fire phenomena, as demonstrated in Figure 3.3(b). Unlike the Zone model, the Field model allows for the consideration of complex spatial and climatic conditions, thus delivering more detailed results. Initially, fire analysis research heavily relied on the

Zone model. However, recent trends have shifted towards the Field model, owing to its ability to simulate fire situations under various conditions with a higher degree of realism. Accordingly, our study aimed to assess the efficacy of the Field model-based FDS in numerically simulating real fire phenomena. After verifying its appropriateness, it was intended for use in the thermofluid analysis of cable-stayed bridges.

Recent research by Choi (2022) has validated FDS's fire simulations by analyzing flame behavior under wind effects. To confirm flame behavior independent of wind, we compared and analyzed FDS results with previous fire experiment data (Heskestad, 1983; Skarsbø, 2011) and variations in flame height relative to fire intensity. Further, to scrutinize flame behavior under wind conditions, we utilized a formula suggested by AGA (1974) to calculate the flame tilt in relation to wind speed. Subsequently, this data was compared and analyzed against FDS simulation results to note variations in flame tilt for different types of vehicles under various wind speeds.

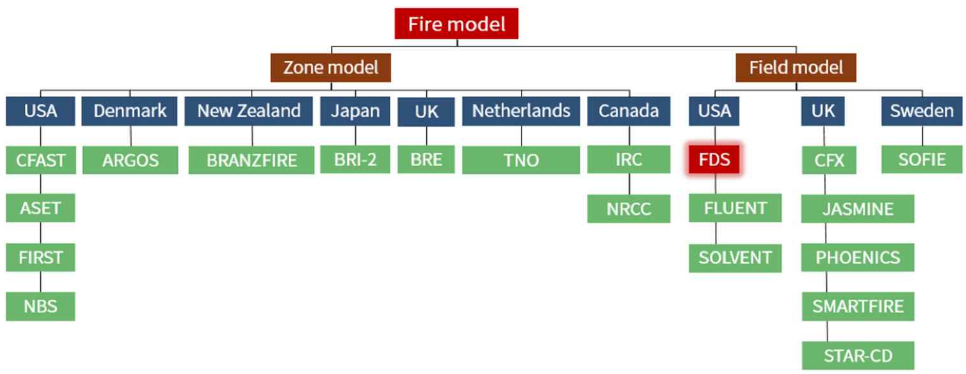

Figure 3.3 Representative Zone and Field models

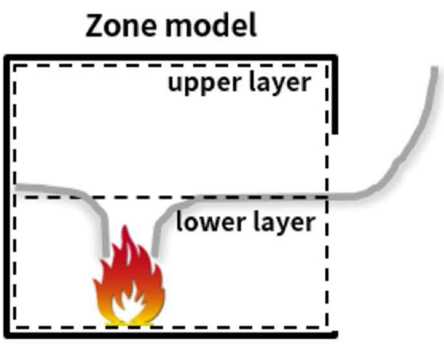

(a) Zone model

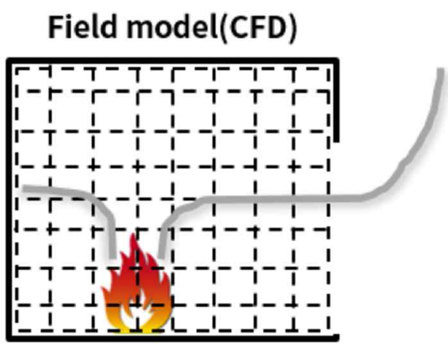

(b) Field model

Figure 3.4 Principles of Zone and Field models

As shown in Figure 3.4, real flames exhibit a distinct temperature distribution pattern, with temperature decreasing towards the flame tip. The FDS simulations mimic these characteristics of real fires, taking into account the properties of the combustion material and the defined fire intensity.

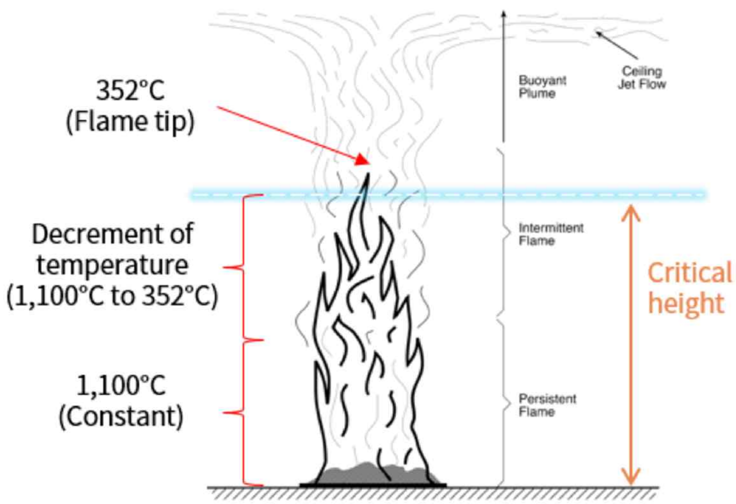

(a) Flame and fire plume (USNRC, 2004)

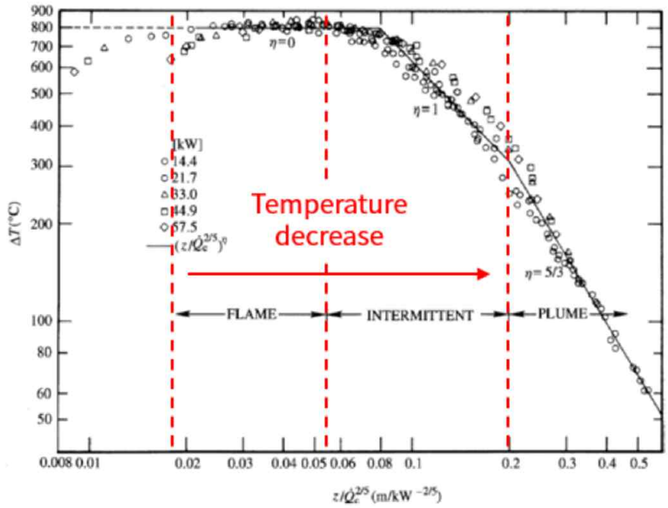

(b) Centerline temperature rise with height in a flame (Drysdale, 2011)

Figure 3.5 Temperature distribution within a flame

(1) Simulation of Fire Uninfluenced by Wind

Choi (2022) utilized the findings from Skarsbø's (2011) actual fire experiment to validate the accuracy of fire simulations that do not take wind effects into account. Figure 3.5 succinctly presents the fire experiment performed by Skarsbø (2011), alongside the Fire Dynamic Simulator (FDS) model created for fire phenomenon validation. The FDS model, used for this validation, incorporated the material properties of Heptane, which was the combustible substance used in Skarsbø's fire experiment. To adequately mimic the fire phenomenon, the fluid domain size was modelled as 1m x 1m x 4m. The model incorporated an element size of 0.025m x 0.025m x 0.025m, with a total of 512,000 elements used. The results of the verification showed a high similarity in flame height between the experimental and analytical scenarios. As illustrated in Figure 3.6, a comparison of temperatures at different flame heights revealed a significant similarity between the temperatures measured in both the experiment and FDS analysis.

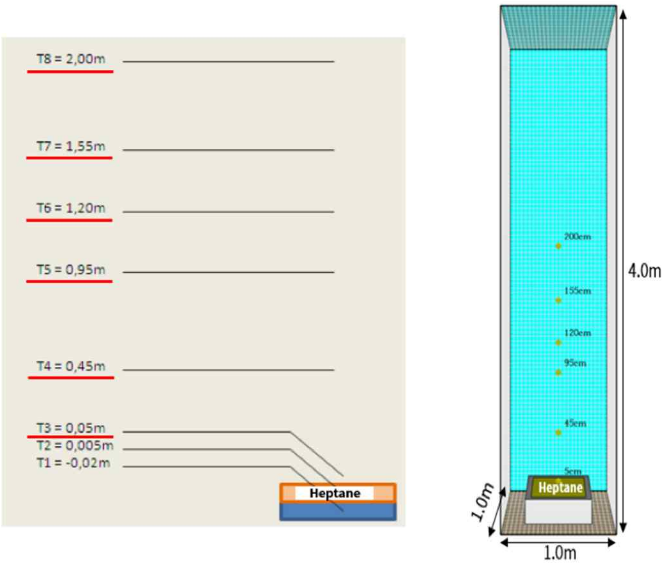

Heptane	
Property	**value**
Emissivity	1.0
Heat of Reaction	318 kJ/kg
Conductivity	0.14 W/m℃
Specific heat	2.24 kJ/kg℃
Density	684 kg/m^3
Absorption coefficient	40 1/m
Boiling Temperature	98.4 ℃
Thickness of fuel layer	0.0152 m

(a) Experiment (b) FDS

Figure 3.6 Fire experiment and FDS Overview

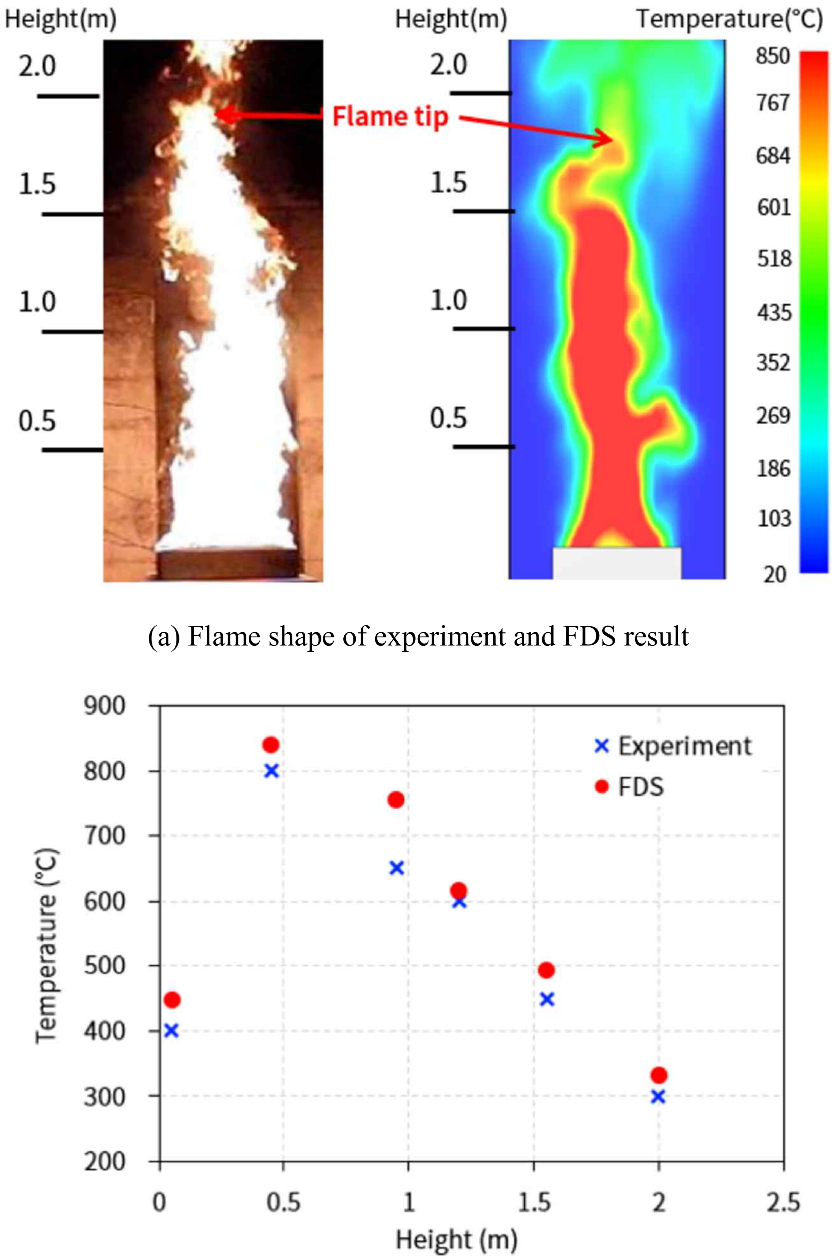

(a) Flame shape of experiment and FDS result

(b) Temperature results at different heights

Figure 3.7 Comparison of fire experiment and FDS results

Heskestad's (1983) formula (equation 3.10) was used to calculate flame height relative to fire intensity, enabling a comparative analysis of flame height as shown in the FDS analysis results and the theoretical flame height based on fire intensity for each vehicle type. Table 3.1 summarizes the flame heights determined by Heskestad's formula and those derived from the FDS analysis for each vehicle type.

Heskestad's (1983) formula (equation 3.10) was used to calculate flame height relative to fire intensity, enabling a comparative analysis of flame height as shown in the FDS analysis results and the theoretical flame height based on fire intensity for each vehicle type. Table 3.1 summarizes the flame heights determined by Heskestad's formula and those derived from the FDS analysis for each vehicle type.

$$H_f = 0.235Q^{2/5} - 1.02D \tag{3.10}$$

Where,

H_f : Flame height (m)

Q : Flame heat release rate (kW)

D : Flame diameter (m)

Table 3.1 Summary of height of flame by Heskestad formula estimation and FDS results

Type	Heskestad formula	FDS
Passenger car	2.75m	2.90m
Bus	5.71m	5.63m
LGV	4.37m	4.1m
HGV	13.82m	13.25m
Tanker	15.36m	14.96m

(2) Simulation of Fire Considering Wind Effects

Flame inclination tends to increase with wind speed. In his recent research, Choi (2022) assessed the FDS's ability to accurately simulate the change in flame inclination under wind effects. This assessment was done by comparing the FDS analysis results with the formula proposed by the American Gas Association (AGA) (1974) (equation 3.11), considering the fire intensity specific to each vehicle type and respective wind speed. Figure 3.7 shows a comparison of flame inclination derived from the AGA calculation and the FDS analysis results, in response to changes in wind speed for each vehicle type. It was found that there was a similar trend across all vehicle types, with flame inclination increasing with wind speed. Notably, in the case of tanker fires, a high degree of congruence was observed between the AGA calculation and the FDS analysis results.

$$\cos\theta = 1 \qquad\qquad , \ u^* \geq 1$$

$$\cos\theta = \frac{1}{\sqrt{u^*}} \qquad\qquad , \ u^* \geq 1$$

Where,

$u^* = \frac{u_w}{(g\dot{m}'' D/\rho_\alpha)^{1/3}}$ (Dimensionless wind speed)

u_w: Wind speed (m/s)

g : 9.81 (m/s^2)

$\dot{m}'$: Mass combustion rate of combustible material (kg/m^{2}s)

D : Flame diameter (m)

ρ_α: Air density (1.225kg/m^3)

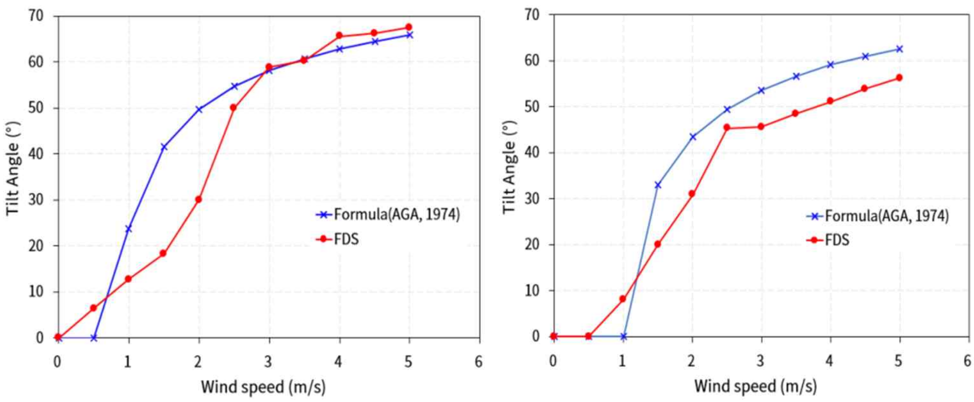

(a) Passenger car (b) Bus

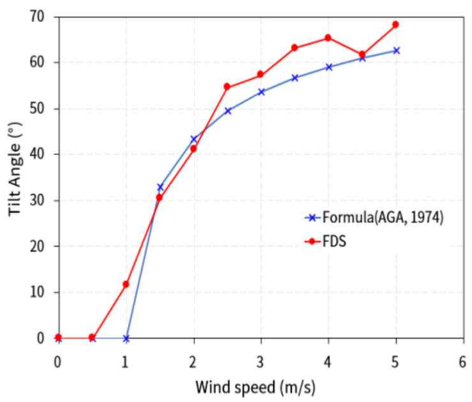

(c) LGV (Light Good Vehicle)

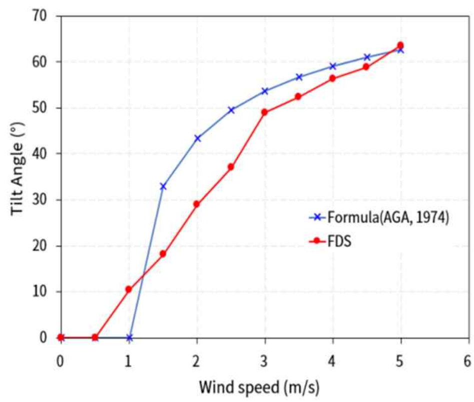

(d) HGV (Heavy Good Vehicle)

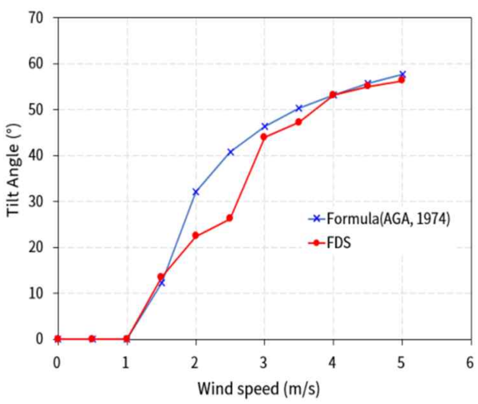

(e) Tanker

Figure 3.8 Tilt angles of flame by AGA formula estimation and FDS results

3.3.2 Numerical Analysis Model

Figure 3.8 illustrates the modeled thermal fluid dynamic analysis domain, which was informed by the Seohae Grand Bridge's structural calculations. The fire-vulnerable segment, characterized by the presence of cables with the maximum cross-sectional area in the central span, was specifically chosen for the evaluation. This numerical analysis model examined the impact of wind conditions on cables 34 to 36 under the presumption of a tanker fire in the selected section.

The size of the fluid domain in the fire-prone segment was set at 34.0m x 36.0m x 14.0m. The element sizes were 0.1m x 0.1m x 0.1m at positions where the highest cable temperature and flame contact were anticipated. In areas where the influence of fire on the cable was projected to be minimal, the elements were modeled at 0.5m x 0.5m x 0.1m. The fire occurrence area, along with all other areas, were set at 0.5m x 0.5m x 0.5m. The total count of elements utilized in each model was approximately 473,328. The thermal properties of cable components, influenced by temperature changes, were determined using the specific heat capacity and thermal conductivity values highlighted in Section 2.4. Figure 3.8 presents the numerical analysis model of the fire-prone segment, prepared for the thermal fluid dynamic analysis.

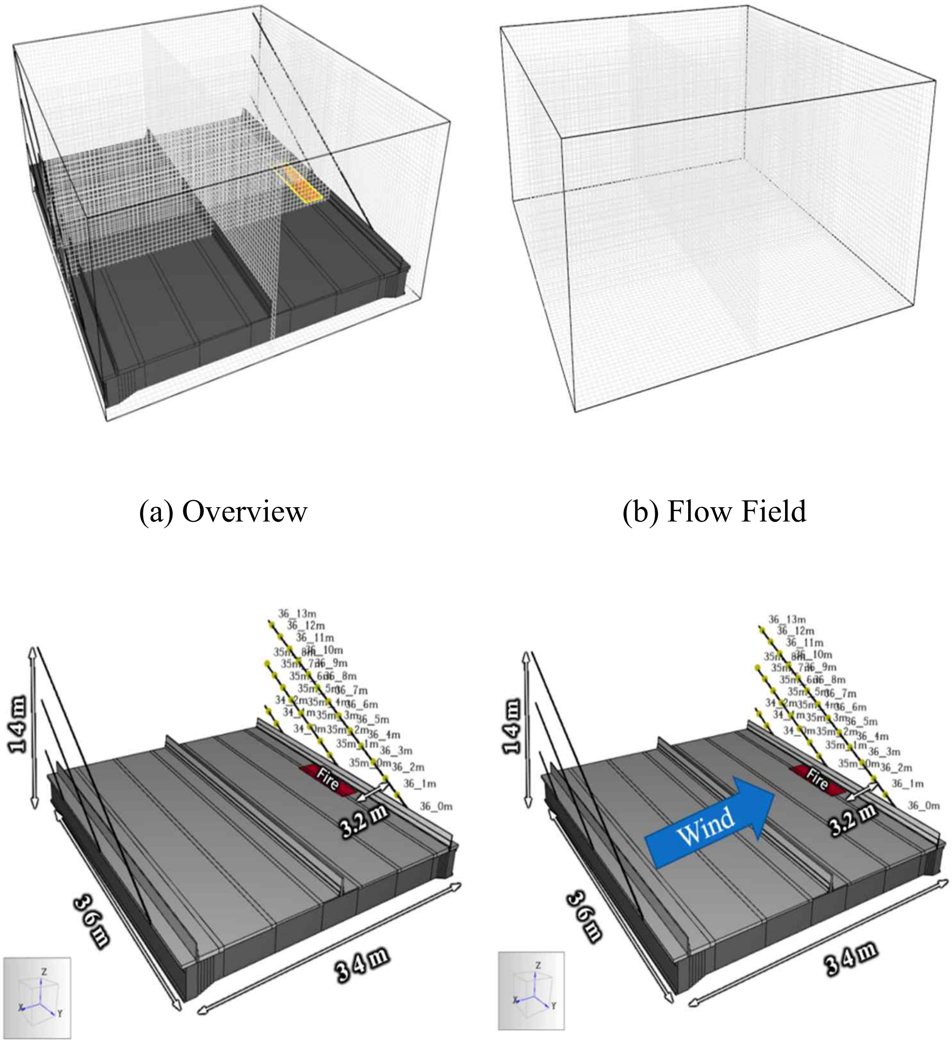

(a) Overview (b) Flow Field

(c) Model without Wind (d) Model with Wind

Figure 3.9 FDS Numerical model

3.3.3 Analysis Conditions

Analysis conditions for the thermal fluid dynamic evaluation were established based on the fire scenarios presented in Chapter 2. The vehicle fire condition factored in the potential of a tanker fire in each lane, irrespective of wind presence, utilizing the fire intensity model proposed in Chapter 2. We operated under the assumption that a vehicle fire would arise in windy conditions, with a wind speed of 3.8 m/s orthogonal to the bridge axis incorporated into the numerical analysis model domain from the upstream side during the pre-fire stage. Thermal fluid dynamic analysis was conducted over a one-hour period to mirror the fire scenario. The analysis conditions are outlined in Figures 3.9 and 3.10. If a vehicle fire transpires on the shoulder, the distance from the center of the fire to the cable is measured at 3.50m

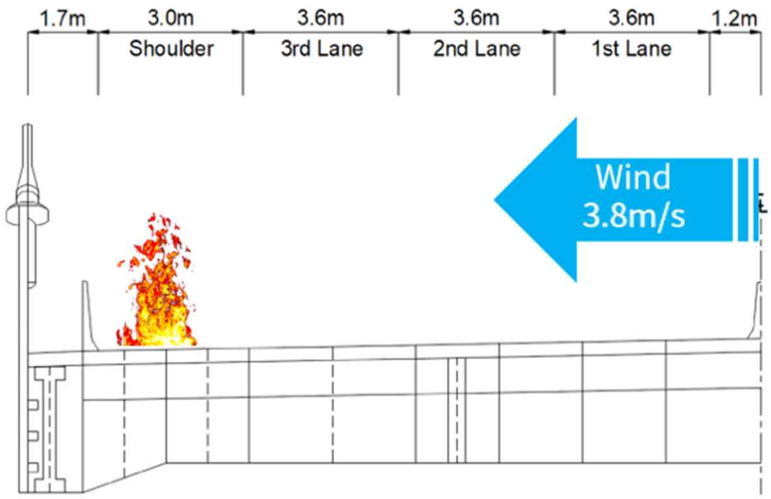

Figure 3.10 Cross-sectional view with wind direction conditions at the fire

location

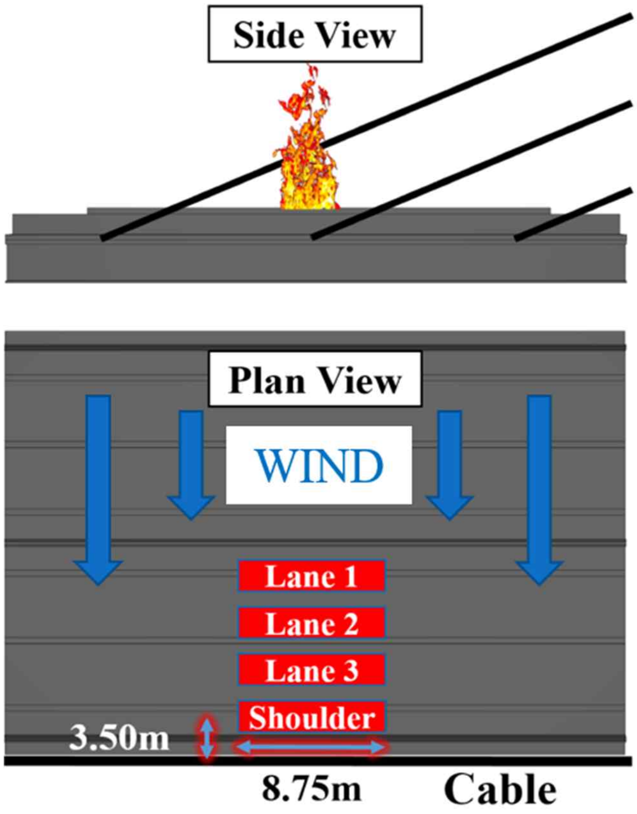

Figure 3.11 Side and plan views with wind direction conditions at the fire location

To assess the wind's effect in the thermal fluid dynamic analysis, temperature changes on the cables were measured. As shown in Figure 3.9, these temperature readings were collected at 1m intervals along the height of the cable.

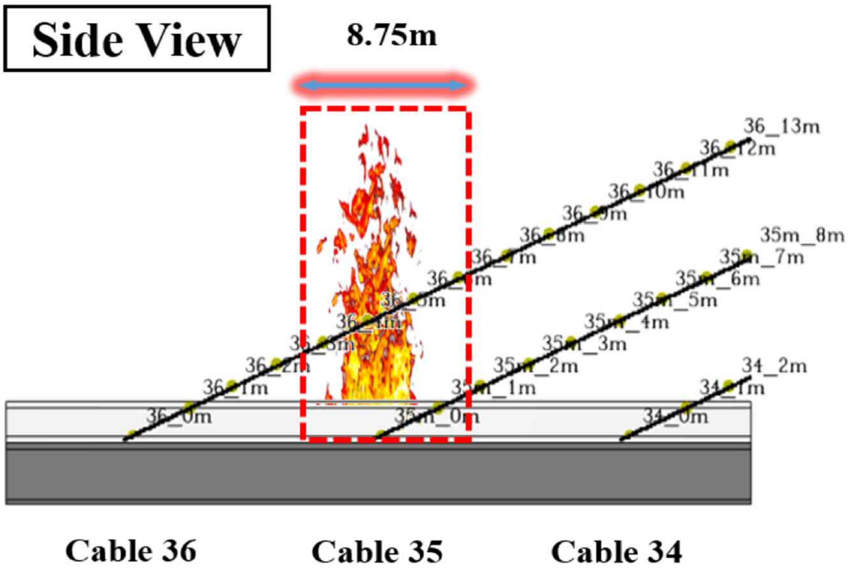

Figure 3.12 Temperature measurement location

3.3.4 Analysis Cases

In this study, the analysis cases align with those outlined in Table 3.2. For scenarios not considering wind effects, the investigations were conducted in relation to tanker fires on the first lane (L1-WO), second lane (L2-WO), third lane (L3-WO), and shoulder lane (SH-WO). In cases incorporating wind, the analysis focused on tanker fires on the second lane (L2-W), third lane (L3-W), and shoulder lane (SH-W). When the influence of wind was considered, the wind speed was set at 3.8m/s. With the wind effect included, there was no instance where the temperature exceeded the 300-degree benchmark, set by

PTI (PTI, 2012), when a tanker fire occurred on the second lane. Therefore, the conditions of a first-lane fire, considering wind effects, were not evaluated.

Table 3.2 Thermal Fluid Analysis Cases

Case	Type of Vehicle	Location (Lane)	Wind Speed (m/s)
SH_No	Tanker	Shoulder	-
L3_No	Tanker	Lane 3	-
L2_No	Tanker	Lane 2	-
L1_No	Tanker	Lane 1	-
SH_Wind	Tanker	Shoulder	3.8
L3_Wind	Tanker	Lane 3	3.8
L2_Wind	Tanker	Lane 2	3.8

CHAPTER 4

THERMAL FLUID ANLYSIS

4.1 Thermal Fluid Analysis Results

This study involved conducting a thermal fluid analysis for vehicle fires occurring in the central span of the Cable-stayed Bridge (Seohae Grand Bridge). The primary variables considered during the analysis were the location of the lane where the vehicle fire occurred and the presence or absence of wind.

As mentioned in Section 3.3.4, the analysis results focus on the 36th cable, where a temperature exceeding the PTI (PTI, 2012) standard was anticipated in the event of a tanker fire. The results for the 34th and 35th cables, not discussed in the main body, have been included in Appendix A. Furthermore, the study analyzed the range of temperature exceedance and flame contact range, as specified by PTI (PTI, 2012), for the targeted cable components.

4.1.1 Results without Wind Effects

Figure 4.1 displays the thermal fluid analysis results for scenarios involving tanker fires on the shoulder, third, second, and first lanes, excluding the impact of wind. In cases where a tanker fire occurs on the first, second, or third lane, the temperature recorded on the cable does not exceed the PTI standard of 300 degrees. However, when a tanker fire takes place on the shoulder lane, the maximum temperature recorded on the cable at a 5m height is approximately 831 degrees. At a height of 6m, the temperature is approximately 575 degrees (refer to Table 4.1). In cases not considering wind, there is no occurrence of flame contact on the cable, regardless of which lane the tanker fire happened.

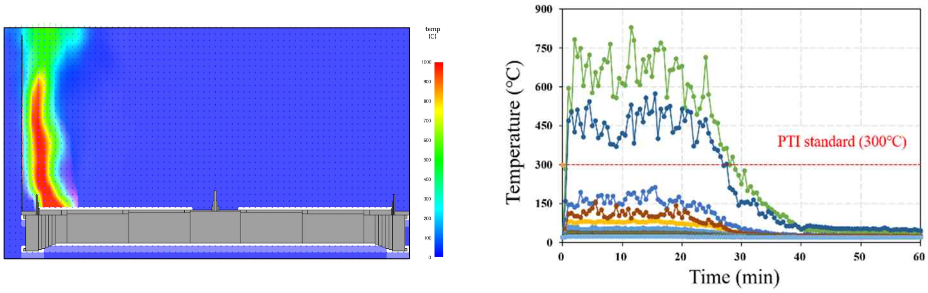

(a) SH_No

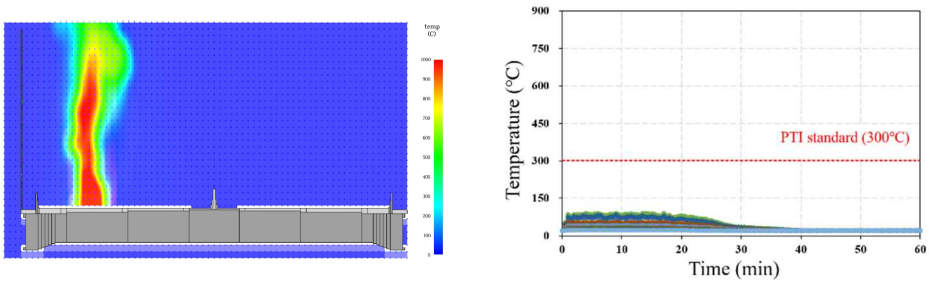

(b) L3_No

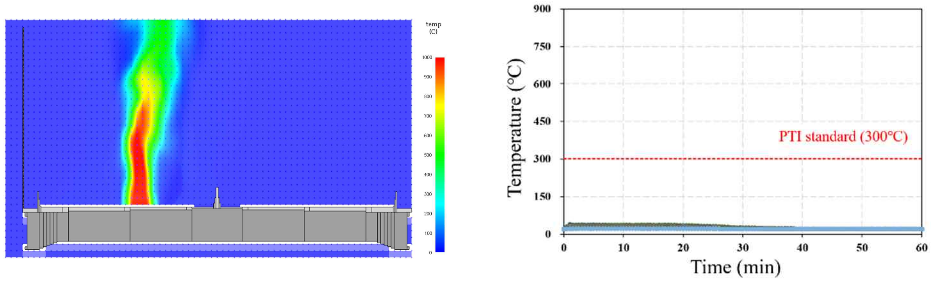

(c) L2_No

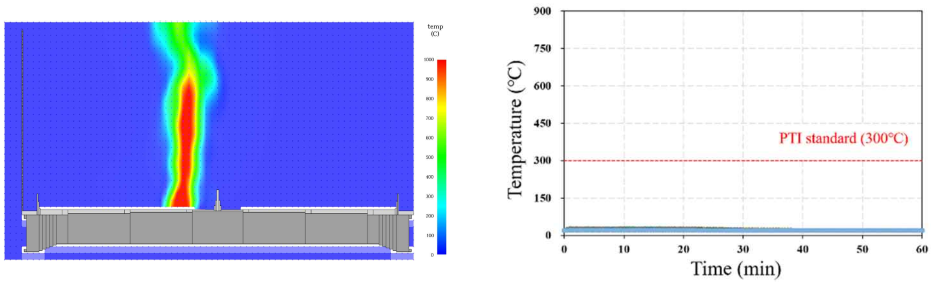

(d) L1_No

Figure 4.1 Thermal fluid analysis results without wind effects (Cable 36)

4.1.2 Results Considering Wind Effects

Figure 4.2 illustrates the thermal fluid analysis results when considering wind effects for tanker fires on the shoulder, third, and second lanes. The figure shows that when a tanker fire takes place on the second lane, the temperature on the cable does not exceed the PTI standard of 300 degrees. However, when a tanker fire happens on the shoulder lane, the temperature recorded on the cable, at heights between 3m and 7m, varies roughly from 433 to 759 degrees (refer to Table 4.1). When a tanker fire occurs on the third lane, the temperature on the cable, at heights between 4m and 6m, lies approximately between 365 and 470 degrees (refer to Table 4.1).

When considering the effect of wind, it has been observed that in the event of a tanker fire on the shoulder of a road, flames reach cables at heights between 2 and 8 meters. However, if such a fire occurs in the third lane, flames make contact with cables located at heights ranging from 3 to 7 meters.

As demonstrated in Table 4.1, when wind effects are factored into a tanker fire occurring on the shoulder, the cables experience higher temperatures compared to scenarios where wind impact is not accounted for. Despite this, the range (height) of cables exceeding the PTI standard of 300 degrees appears to broaden. In the absence of wind, temperatures on the cable during a third-lane fire remain below 300 degrees. Nevertheless, when the influence of wind is considered, temperatures on the cable exceed this threshold.

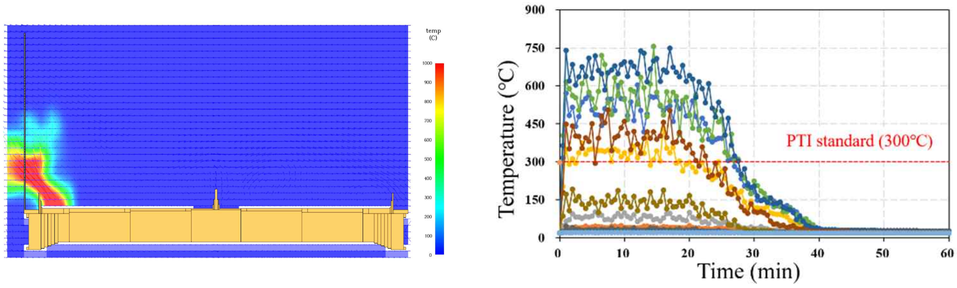

(a) SH_Wind

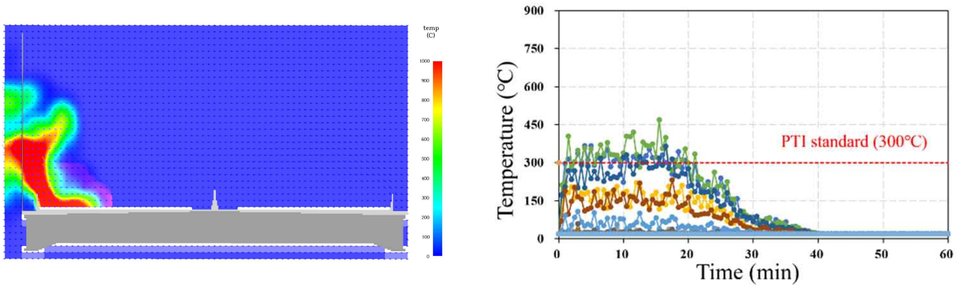

(b) L3_Wind

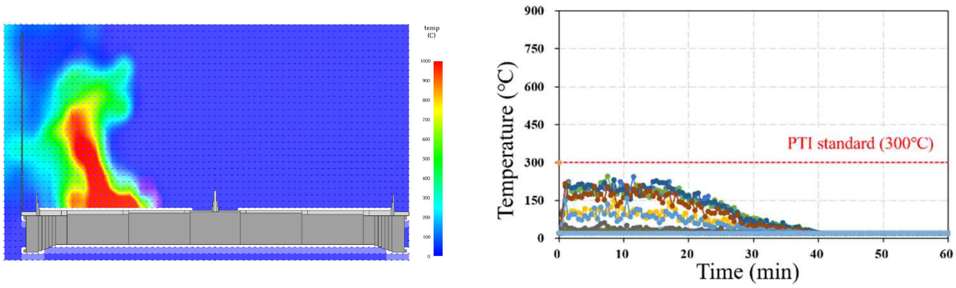

(c) L2_Wind

Figure 4.2 Thermal fluid analysis results with wind effects (Cable 36)

Table 4.1 Maximum temperature reached at various cable heights during an tanker fire in different lanes.

(a) Without wind

Height of Cable	Shoulder (No. of Cable)			Lane 3 (No. of Cable)			Lane 2 (No. of Cable)			Lane 1 (No. of Cable)		
	34	35	36	34	35	36	34	35	36	34	35	36
1m	24	144	34	23	59	30	22	33	25	21	26	22
2m	23	71	48	22	51	40	22	32	29	21	25	24
3m	-	47	84	-	39	55	-	29	33	-	24	26
4m	-	38	213	-	32	74	-	26	37	-	24	27
5m	-	31	**831**	-	27	90	-	24	39	-	23	28
6m	-	28	**575**	-	25	83	-	23	37	-	22	27
7m	-	25	157	-	23	54	-	22	33	-	22	26
8m	-	23	61	-	22	42	-	22	29	-	21	25
9m	-	-	41	-	-	33	-	-	27	-	-	24
10m	-	-	33	-	-	29	-	-	26	-	-	23
11m	-	-	28	-	-	26	-	-	24	-	-	22
12m	-	-	25	-	-	24	-	-	23	-	-	22
13m	-	-	24	-	-	22	-	-	22	-	-	21

(b) With wind

Height of Cable	Shoulder (No. of Cable)			Lane 3 (No. of Cable)			Lane 2 (No. of Cable)		
	34	35	36	34	35	36	34	35	36
1m	24	267	48	20	66	22	23	75	29
2m	22	192	104	20	196	43	23	89	38
3m		64	**433**	-	164	221	-	46	150
4m	-	36	**606**	-	34	**367**	-	31	243
5m	-	29	**759**	-	22	**470**	-	25	246
6m	-	26	**750**	-	20	**365**	-	24	232
7m	-	23	**507**	-	20	233	-	22	218
8m	-	22	195	-	20	108	-	21	159
9m	-	-	46	-	20	59	-	-	62
10m	-	-	28	-	-	32	-	-	30
11m	-	-	25	-	-	20	-	-	24
12m	-	-	23	-	-	20	-	-	22
13m	-	-	21	-	-	20	-	-	21

4.2 Summary and Analysis Results

In scenarios that discount the influence of wind, no contact is observed between the flame and the cable across all lanes during a tanker fire. As a result, it can be inferred that fire-resistant measures are only necessary when a tanker fire occurs on the shoulder, assuming the impact of wind is not considered.

Conversely, when the effects of wind are factored in, the maximum temperature recorded on the cable is somewhat lower compared to scenarios where wind effects are disregarded (as shown in Table 4.1). Nevertheless, the range (height) exceeding the PTI standard of 300 degrees expands. As in earlier findings, temperatures on the cable during a third-lane fire stay below 300 degrees in the absence of wind. Yet, when wind impact is taken into account, the temperatures on the cable surpass this limit. As a result, it is proposed that fire-resistant measures are necessary during tanker fires on both the shoulder and the third lane, provided the effect of wind is considered. Furthermore, the study suggests an increase in the scope requiring fire-resistant measures compared to situations where wind effects are not considered.

This research evaluates the temperatures occurring on the cable during a vehicular fire on the Seohae Grand Bridge, with considerations for the presence or absence of wind. The methodology employed for evaluating temperatures during a vehicle fire on cable-stayed bridges could be effectively applied to conduct thermal fluid dynamics analyses on other cable-stayed bridge types with different component configurations. It is anticipated that this approach would enable a more accurate estimation of temperature occurrence based on component arrangement, thereby facilitating a more precise evaluation of the range requiring fire-resistant measures for each type of cable-stayed bridge.

CHAPTER 5

CONCLUSIONS

This research presents an evaluation of temperature fluctuations within the cables of the Seohae Grand Bridge during a vehicle fire, considering the potential effects of wind. The implementation of thermal fluid analysis facilitated the derivation of the temperature-time history of the cables, which enabled an examination of the maximum temperatures, exceedance of temperature benchmarks, flame contact range, and wind's impact on the lanes affected by the vehicle fire.

The analysis was conducted primarily on the central interval of the bridge, where a broad range encompassing the suspender assemblies fell within the fire's reach. This corresponded to cases where the suspender placement angle was relatively low. Therefore, it is anticipated that conducting thermal fluid analyses for sections with higher suspender placement angles during a vehicle fire could result in more effective fire-resistant strategies for those specific segments. The principal conclusions drawn from the study are as follows:

In scenarios where the wind's impact was not factored in, there was no observed flame contact with the cables during tanker fires in any of the lanes. However, when a tanker fire occurred on the shoulder, the maximum temperature experienced by the cables surpassed the Post-Tensioning Institute (PTI) standard of 300 degrees. As a result, it is inferred that fire-resistant measures may be necessary for tanker fires occurring on the shoulder when wind impact is not considered.

When considering the effects of wind, the maximum temperatures recorded by the cables were lower than when wind's influence was disregarded. Nevertheless, the height at which the cables exceeded the PTI standard of 300 degrees exhibited an increase. When wind effects were not considered, temperatures on the cable during a third-lane fire remained below 300 degrees. However, under the influence of wind, temperatures on the cables exceeded this threshold. As a result, it is suggested that fire-resistant measures should be implemented in situations where a tanker fire occurs on the shoulder or the third lane, particularly when wind impact is considered. In addition, the research indicates an expanded scope requiring fire-resistant measures when compared to situations where the effects of wind are disregarded.

The methodology employed in this study for temperature evaluation during a vehicle fire on cable-stayed bridges could serve as an effective tool for thermal fluid dynamics analyses across different cable-stayed bridge designs with diverse suspender arrangements. This approach is expected to facilitate a precise estimation of temperature variations and allow a more accurate assessment of the areas requiring fire-resistant measures for each type of cable-stayed bridge.

The results of this study can provide valuable evaluation data that will inform the development of fire-resistant strategies and help define the range for fire reinforcement of cables, thereby preparing for potential vehicle fires on cable-stayed bridges.

REFERENCE

Enforcement Decree of the Building Act, Articles 56 and 57 (Presidential Decree No. 32411, February 11, 2022).

Ministry of Land, Infrastructure, and Transport. (2016). Road bridge design standards (Limit state design method).

Ministry of Land, Infrastructure, and Transport. (2016). Road bridge design standards (Limit state design method) - Cable-stayed bridges.

Ministry of Land, Infrastructure, and Transport. (2016). Guidelines for the installation and management of disaster prevention facilities in road tunnels.

Ministry of Land, Infrastructure, and Transport. (2016). Guidelines for the design of underground roads in urban areas.

Ministry of Land, Infrastructure, and Transport. (2021). Land, Infrastructure, and Transport statistical yearbook.

Ministry of Land, Infrastructure, and Transport. (2021). Road structure rule (Ministry of Land, Infrastructure, and Transport Notification No. 922, December 13, 2021).

Ministry of Land, Infrastructure, and Transport. (2021). Guidelines for fire protection in road tunnels.

National Fire Agency. (2017). Fire safety standards for road tunnels (NFSC 603).(NFSC 603).

National Fire Agency. (2018). Fire statistics yearbook 2018.

Korea Expressway Corporation. (2013). Guidelines for fire-resistant design and construction of tunnels.

Korea Expressway Corporation. (2014). Guidelines for fire-resistant design of highway bridge substructures.

Korea Expressway Corporation. (2014). Guidelines for evaluating fire risk for highway bridges.

Korea Expressway Corporation. (2018). Research on fire protection and blast resistance measures for tunnel bridges subjected to vehicle fires (Research Report).

Korea Expressway Corporation. (2020). Stability evaluation of the Seohae Grand Bridge based on field measurements and research on disaster response measures (Research Report).

Korean Institute of Bridge Structural Engineers. (2021). Evaluation of cable-stayed bridge systems subject to special loads (fire and explosion).

ACI Committee 216 (1989). Guide for Determining the Fire Endurance of Concrete Elements. ACI 216R-89, Detroit, USA.

ACI Committee 216 (2007). Code Requirements for Determining Fire Resistance of Concrete and Masonry Construction Assemblies. ACI 216.1/TMS-0216, Detroit, USA.

Albero, V., Serra, E., Espinos, A., Romero, M.L. and Hospitaler, A. (2021). Internally fire protected composite steel-concrete slim-floor beam. Engineering Structures, 227, 111447:1-11.

Alnahhal, W. I., Chiewanichakorn, M., Aref, A. J. and Alampalli, S. (2006). Temporal Thermal Behavior and Damage Simulations of FRP Deck. Journal of Bridge Engineering, 11(4), 452-464.

American Gas Association(AGA) (1974). LNG Safety Research Program. Report IS 3-1.

American Society of Civil Engineers(ASCE) (1980). Structural Analysis and Design of Nuclear Plant Facilities. ASCE, New York, USA.

American Society for Testing and Materials(ASTM) (2000). Standard Methods of Fire Tests of Building Construction and Materials. ASTM E119-82, Philadelphia, USA.

Ariyanayagam, A. D. and Mahendran, M. (2019). Influence of cavity insulation on the fire resistance of light gauge steel framed walls. Construction and Building Materials, 203, 687-710.

BABS (1967). Svensk ByggNorm 67. Sweden.

Baker, C. (2015). Risk analysis of pedestrian and vehicle safety in windy environments. Journal of Wind Engineering and Industrial Aerodynamics, 147, 283-290.

CETU (2002). Centre d’ Etudesdes Tunnel(Tunnel Design Center). France.

Chen, J., Hamed, E. and Gilbert, R. I. (2021). Structural performance of concrete sandwich panels under fire. Fire Safety Journal, 121, 103293:1-15.

Chung, C., Choi, H. S., & Lee, J. (2019). Investigation of temperature variation of bridge cables under fire hazard using heat transfer analysis. Journal of the Computational Structural Engineering Institute of Korea, 32(5), 313–322. (In Korean).

Cui, C., Chen, A. and Ma, R. (2020). Stability assessment of a suspension bridge considering the tanker fire nearby steel-pylon. Journal of Constructional Steel Research, 172, 106186:1-9.

Drysdale, D. (2011). An Introducion to Fire Dynamics(3rd edition). Wiley.

Duan, J. D., Xiao, J., Zhang, D., Zheng, W. and Zhang, S. (2021). A large-scale fire test of an immersed tunnel under the protection of fire resistive coating. Tunnelling and Underground Space Technology incorporating Trenchless Technology Research, 111, 103844:1-22.

Dymat Construction Products, Inc. (2018) Systems and Methods for Fireproofing Cables and Other Structural Members (U.S. Patent No. 10,512,803 B2). Washington, DC: U.S. Patent and Trademark Office.

EIFFAGE TP. (2007) Device for Protecting a Cable or the Like of a Construction or Civil Engineering Project from Fire (WO Patent No. 2007/093703 A2). PTC World Intellectual Property Organization.

European Committee for Standardization(CEN) (2002). EUROCODE 1: Action on Structures Part 1-2: General Actions, Actions on Structures Fire Design(EN 1991-1-2). CEN, Brussels, Belgium.

European Committee for Standardization(CEN) (2005). EUROCODE 3: Design of Steel Structures Part 1-2: General Rules, Structural Fire Design(EN 1993-1-2). CEN, Brussels, Belgium.

Freyssinet International. (2001). Anchoring Device for Fixing a Structural Cable to a Building Element (U.S. Patent No. 6,578,329 B1). Washington, DC: U.S. Patent and Trademark Office.

Garlock, M., Paya-Zaforteza, I., Kodur, V. and Gu, L. (2012). Fire hazard in bridges: Review, assessment and repair strategies. Engineering Structures, 35, 89-98.

Gong, X. and Agrawal, A. K. (2015). Safety of Cable-Supported Bridges during Fire Hazards. Journal of Bridge Engineering, 21(4), 04015082:1-12.

Heselden, A. (1976). Studies of Fire and Smoke Behavior Relevant to Tunnel. Proceeding of the 2nd international Symposium Aerodynamics & Ventilation of Vehicle Tunnels, 23-25 March, 1976, Cambridge, UK

Hesekestad, G. (1983). Luminous Height of Turbulent Diffusion Flames. Fire Safety Journal, 5(2), 103-108.

Hsu, W.-S., Huang, Y.-H., Shen, T.-S., Cheng, C.-Y. and Chen, T.-Y. (2017). Analysis of the Hsuehshan Tunnel Fire in Taiwan. Tunneling and Underground Space Technology, 69, 108-115.

Ingason, H., Gustavsson, S. and Dahlberg, M. (1994). Heat Release Rate Measurements in Tunnel Fires. SP Report 1994:08, Swedish National Testing and Research Institute.

Ingason, H. and Lönnermark, A. (2005). Heat release rates from heavy goods vehicle trailer fires in tunnels. Fire Safety Journal, 40(7), 646-668.

Ingason, H. and Li, Y. Z. (2017). Spilled liquid fires in tunnels. Fire Safety Journal, 91, 399-406.

International Tunnelling Association(ITA) (2004). Guidelines for Structural Fire Resistance for Road Tunnels. ITA.

International Tunnelling Association(ITA) (2017). Structural Fire Protection for Road Tunnels. ITA.

ISO (1999). Fire-resistance tests-Elements of building construction-Part 1: General requirements. International Standard ISO 834, Geneva.

Jensen, J. L., Narasimhan, H., Giuliani, L. and Jomaas, G. (2019). Development of fire protection for bridge cable systems. The 14th Nordic Steel Construction Conference, 18-20, September, 2019, Copenhagen, Denmark.

Karlsson, B. and Quintiere, J. G. (2000). Enclosure fire dynamics 693, CRC Press.

Kim M. O., Kim, K., Yun, J. H. and Kim, M. K. (2020). Fire risk assessment of cable bridges for installation of firefighting facilities. Fire Safety Journal, 115, 103146:1-9.

Kim, S. (2011). A Study on Fire-resistant Facilities for Cable Bridges in the Event of Cable Bridge Fires (Master's thesis, Jeonju University).

Kim, S., Shim, J., Rhee, J. Y., Jung, D. and Park, C. (2019). Temperature Distribution Characteristics of Concrete during Fire Occurrence in a Tunnnel. applied sciences, 9, 4740:1-11.

Kodur, V. K., Aziz, E. M. and Naser, M. Z. (2017). Strategies for enhancing fire performance of steel bridges. Engineering Structures, 131, 446-458.

Kodur, V.K.R. and Naser, M.Z. (2019). Designing steel bridges for fire safety, Journal of Construction Steel Research, 156, 46-53.

Kolaitis, D., Asimakopoulou, E. K. and Founti, M. A. (2014). Fire protection of light and massive timber elements using gypsum plasterboards and wood based panels: A large-scale compartment fire test. Construction and Building Materials, 73, 163-170.

Kragh, E., Narasimhan, H. and Jensen, J. L. (2018). Fire protection of suspension bridge main cables. IABSE Conference 2018 – Engineering the Past, to Meet the Needs of the Future, 25-27 June, 2018, Copenhagen, Denmark.

Kragh, E., Narasimhan, H. and Jensen, J. L. (2020). Fire Protection of Bridge Cables. Structural Engineering International, 30(4), 530-533.

Kunikane, Y., Kawabata, N., Ishikawa, T., Takekuni, K. and Shimoda, A. (2002). Thermal fumes and smoke induced by bus fire accident in large corss sectional tunnel. The 5th JSME-KSME Fluids Engineering Conference, 17-21 November, 2002, Nagoya, Japan.

Lie, T. T. (1992). Structural Fire Protection. ASCE Manual and Reports of Engineering Practice No.78, ASCE, New York, USA.

Liu, Y., Lou, G., Ju, X. and Liu, X. (2017). Safety evaluation of a large-span double-deck cable-stayed steel bridge under fire. The 8th European Conference on Steel and Composite Structures, 13-15, September, 2017, Copenhagen, Denmark.

Magarabooshanam, H., Ariyanayagam, A. and Mahendran, M. (2019). Behaviour of load bearing double stud LSF walls in fire. Fire Safety Journal, 107, 15-28.

Mangs, J. and Keski-Rahkonen, O. (1994a). Characterization of the Fire Behavior of a Burning Passenger Car. Part I: Car Fire Experiments. Fire Safety Journal, 23(1), 17-35.

Mangs, J. and Keski-Rahkonen, O. (1994a). Characterization of the Fire Behavior of a Burning Passenger Car. Part II: Parametrization of Measured Rate of Heat Release Curves. Fire Safety Journal, 23(2), 37-49.

Ma, R., Chuanjie, C., Minglei, M. and Airong, C. (2019). Performance-based design of bridge structures under vehicle-induced fire accidents: Basic framework and a case study. Engineering structures, 197, 109390:1-13.

Monckton, H. (2018). Practical design, testing & verification guidelines for pre-cast segmental tunnel linings subjected to fire loading. Tunneling and Underground Space Technology, 77, 237-248.

Munson, D. and Decker, D. (2012). Fire testing of high density polyethylene piping systems. ASME 2012 Pressure Vessels and Piping Conference, 15-19, July, 2012, Toronto, Ontario, Canada.

Narasimhan, H., Giuliani, L., Jomaas, G. and Jensen, J. L. (2019). Fire risks in suspension bridges. The 14th Nordic Steel Construction Conference, 18-20, September, 2019, Copenhagen, Denmark.

National Fire Protection Association(NFPA) (2017). Standard for Road Tunnels, Bridges, and Other Limited Access Highways. NFPA 502,

New York State Department of Transportation(NYSDOT) (2017). NYSDOT-bridge failure data base. NYSDOT, New York, USA.

NIST (2021) Fire Dynamics Simulator User's Guide 6th edition, National Institute of Standards and Technology.

Payá-Zaforteza, I. and Garlock, M.E.M. (2012). A numerical investigation on the fire response of a steel girder bridge. Journal of Construction Steel Research, 75, 93-103.

Perera, D., Poologanathan, K., Gillie, M., Gatheeshgar, P., Sherlock, P., Nanayakkara, S.M.A. and Konthesingha, K.M.C. (2020). Fire performance of cold, warm and hybrid LSF wall panels using numerical studies. Thin-Walled Structures, 157, 107109:1-13.

Perera, D., Poologanathan, K., Gatheeshgar, P., Upasiri, I. R., Sherlock, P., Rajanayagam, H. and Nagaratnam, B. (2021). Fire performance of modular wall panels: Numerical analysis. Structures, 34, 1048-1067.

Peris-Sayol, G., Paya-Zaforteza, I., Alos-Moya, J. and Hospitaler, A. (2015). Analysis of the influence of geometric, modeling and environmental parameters on the fire response of steel bridges subjected to realistic fire scenarios. Computers and Structures, 158, 333-345.

PTI (2012) PTI DC45.1.1-12: Recommendations for Stay-Cable Design, Testing, and Installation, PTI, Farmington Hills, MI.

RABT (2006). Richtilinien fur die Ausstattung und den Betrieb con Straßentunneln. RABT

Randaxhe, J., Popa, N., Vassart, O. and Tondini, N. (2021). Development of a plug-and-play fire protection system for steel columns. Fire Safety Journal, 121, 103272:1-26.

Rusthi, M., Ariyanayagam, A., Mahendran, M. and Keerthan, P. (2017). Fire tests of Magnesium Oxide board lined light gauge steel frame wall systems. Fire Safety Journal, 90, 15-27.

Skarsbø, L. R. (2011). An Experimental Study of Pool Fires and Validation of Different CFD Fire Models. University of Bergen, Master thesis.

SOBEN INTERNATIONAL (2019). Fire Resisting Construction Solutions & Technical Manual, Concrete & Tunnel Structures.

SOLETANCHE FREYSSINET. (2012). Structural Cable with Fire Protection (WO 2012/052796 A1). PTC World Intellectual Property Organization.

Tao, Y. and Mahendran, M. (2021). Fire tests and thermal analyses of LSF walls insulated with sulica aerogel fibreglass blanket. Fire Safety Journal, 122, 103352:1-16.

Timilsina, S., Yazdani, N. and Beneberu, E. (2021). Post-fire analysis and numerical modeling of a fire-damaged. Engineering Structures, 244, 112764:1-11.

Tolstrup, J., Giuliani, L., Narasimhan, H., Jensen, J. L. and Jomaas, G. (2019). Experimental study of epoxy coatings for fire protection of bridge cables. The 14th Nordic Steel Construction Conference, 18-20, September, 2019, Copenhagen, Denmark.

Triantafillou, T. C., Karlos, K., Kefaou, K. and Argyropoulou, E. (2017). An innovative structural and energy retrofitting system for URM walls using textile reinforced mortars combined with thermal insulation: Mechanical and fire behavior. Construction and Building Materials, 133, 1-13.

United States Nuclear Regulatory Commission(USNRC) (2004). Fire Dynamics Tools(FDTs): Quantitative Fire Hazard Analysis Methods for the U.S. Nuclear Regulatory Commission Fire Protection Inspection Program. NUREG-1805, Washington, USA.

Wang, L. L., Wang, Y. C., Li, G. Q. and Zhang, Q. Q. (2020). An experimental study of the effects of topcoat on aging and fire protection properties of intumescent coatings for steel elements. Fire Safety Journal, 111, 102931:1-9.

Wang, Y., Burgess, I., Wald, F. and Gillie, M. (2017). Performance-based Fire Engineering of Structures. CRC Press.

World Road Association(PIARC) (2002). PIARC Proposal on the Design Criteria for Re-sistance to Fire for Road Tunnel Structures. PIARC.

World Road Association(PIARC) (2007). Fire and Smoke Control in Road Tunnels. PIARC.

Wu, X.-Q., Huang, T. and Au, F. T. K. (2020). A Localized Fire Model for Predicting the Surface Temperature of Box Girder Bridges Subjected to Tanker Truck Fire. Fire Technology, 56, 2059-2087.

Xu, C. and Liu, Z. (2022). Coupled CFD-FEM Simulation of Steel Box Bridge Exposed to Fire. Advances in Civil Engineering, 2022, 5889743:1-12.

APPENDIX

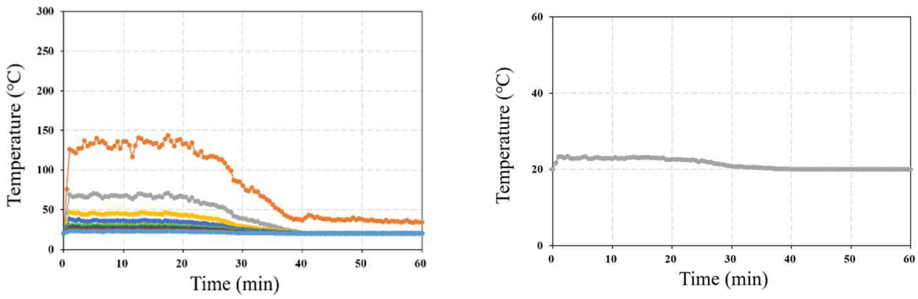

(a) SH_No: Cable 35 and Cable 34

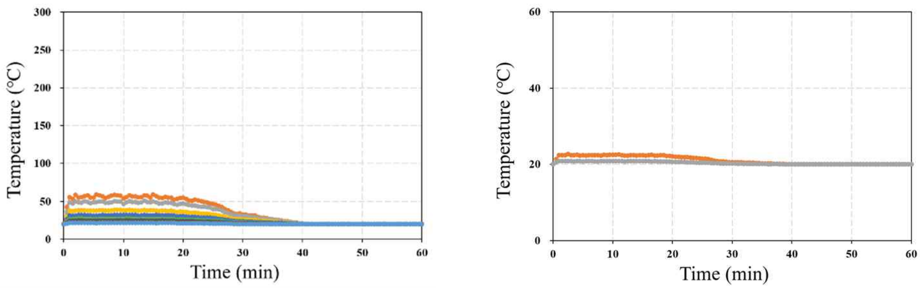

(b) L3_No: Cable 35 and Cable 34

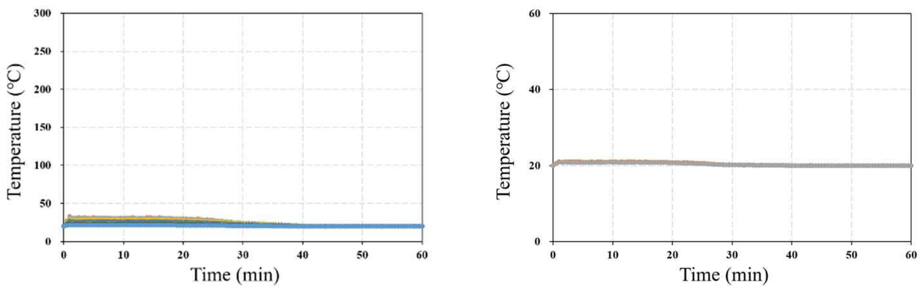

(c) L2_No: Cable 35 and Cable 34

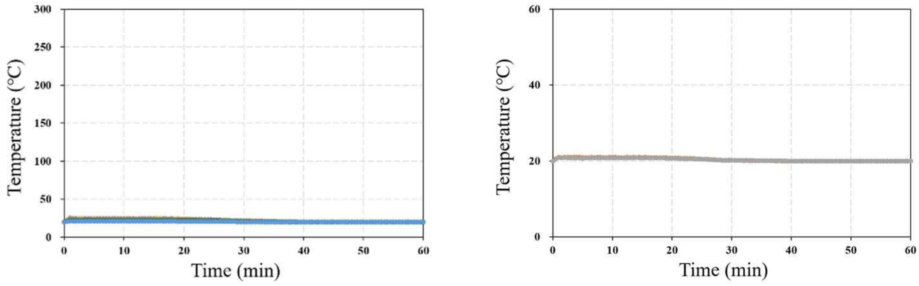

(d) L1_No: Cable 35 and Cable 34

Figure A.1 Thermal fluid analysis results without wind effects

(Cables 34 & 35)

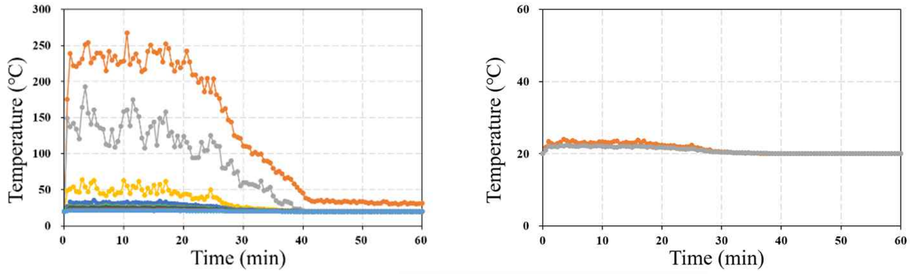

(a) SH_Wind: Cable 35 and Cable 34

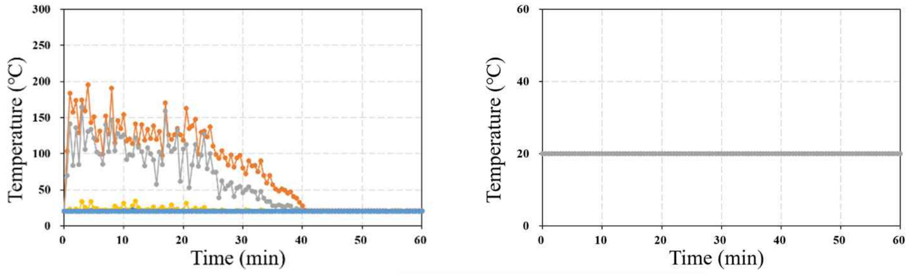

(b) L3_Wind: Cable 35 and Cable 34

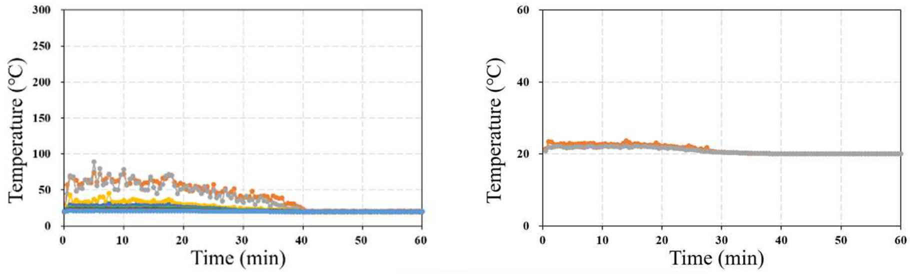

(c) L2_Wind: Cable 35 and Cable 34

Figure A.2 Thermal fluid analysis results with wind effects

(Cables 34 & 35)

국 문 초 록

정 우 진
건설환경공학부
서울대학교 대학원

지진 및 태풍과 같은 자연재난에 대해서는 케이블 교량에 대한 설계기준이나 대책 방안을 마련하고 있지만, 케이블 교량에서 발생하는 차량화재에 대한 평가 기준 및 지침은 연구가 미흡한 실정이다. 케이블 교량 상부에서 발생하는 차량화재는 개방형 환경에서의 화재이며, 화재 발생 시 바람의 영향을 크게 받는다. 따라서 케이블 교량 상에서 차량화재에 의한 열 유동 평가 시에는 이들 요인이 고려되어야 한다. 케이블 교량(사장교)상에서 차량화재 발생 시에는 바람의 영향 유무는 케이블 부재에서의 발생 온도의 크기 및 범위에 큰 영향을 미칠 것으로 판단된다. 기존에 사장교를 대상으로 차량 화재에 의한 화재해석 연구가 수행된 예가 있으나 바람의 영향을 고려한 연구는 이루어지지 않았다.

본 연구에서는 사장교를 대상으로 바람의 영향을 고려한 열 유동 해석을 수행하여 차량 화재에 대한 케이블의 온도 변화 및 기준 초과 범위를 분석하였다. 또한, 바람의 영향 고려 유무에 따른 발생 온도를 비교 및 분석하였다. 열 유동 해석에 필요한 화재 강도, 시나리오 설정 및 온도에 따른 케이블 부재의 재료 특성 변화를 고려하였으며, 평가

기준은 PTI(PTI, 2012) 기준을 참고하여 기준 초과 범위를 분석하였다. 화재 시나리오 설정 시 대상 교량의 취약 구간, 평균 풍속 값 및 화재 진압 시간 등을 고려하였으며, 화재 강도 모델은 개방형 환경인 사장교에서 발생하는 차량 화재에 적합한 화재 강도모델을 조사하여 이용하였다. 열 유동 해석결과, 바람의 영향을 고려하는 경우에는 기준을 초과하는 화재 발생 차선 및 케이블의 평가기준 온도의 초과 범위가 확대되는 것을 확인하였다.

주요어: 사장교; 열유동해석; 차량화재; 화재해석;

Student Number: 2019-20019